



HAL
open science

Caspartin and calprismín, two proteins of the shell calcitic prisms of the Mediterranean fan mussel *Pinna nobilis*.

Frédéric Marin, Reinout Amons, Nathalie Guichard, Martin Stigter, Arnaud Hecker, Gilles Luquet, Pierre Layrolle, Gérard Alcaraz, Christophe Riondet, Peter Westbroek

► To cite this version:

Frédéric Marin, Reinout Amons, Nathalie Guichard, Martin Stigter, Arnaud Hecker, et al.. Caspartin and calprismín, two proteins of the shell calcitic prisms of the Mediterranean fan mussel *Pinna nobilis*. Journal of Biological Chemistry, 2005, 280 (40), pp.33895-908. 10.1074/jbc.M506526200 . inserm-00166083

HAL Id: inserm-00166083

<https://inserm.hal.science/inserm-00166083>

Submitted on 31 May 2020

HAL is a multi-disciplinary open access archive for the deposit and dissemination of scientific research documents, whether they are published or not. The documents may come from teaching and research institutions in France or abroad, or from public or private research centers.

L'archive ouverte pluridisciplinaire **HAL**, est destinée au dépôt et à la diffusion de documents scientifiques de niveau recherche, publiés ou non, émanant des établissements d'enseignement et de recherche français ou étrangers, des laboratoires publics ou privés.

Copyright

Caspartin and Calprismin, Two Proteins of the Shell Calcitic Prisms of the Mediterranean Fan Mussel *Pinna nobilis**

Received for publication, June 15, 2005, and in revised form, June 30, 2005 Published, JBC Papers in Press, July 1, 2005, DOI 10.1074/jbc.M506526200

Frédéric Marin^{†§1}, Reinout Amons^{||}, Nathalie Guichard[‡], Martin Stigter[§], Arnaud Hecker^{†**}, Gilles Luquet[‡], Pierre Layrolle[§], Gérard Alcaraz^{††}, Christophe Riondet^{††}, and Peter Westbroek^{§§}

From the [†]UMR CNRS 5561 "Biogéosciences," Université de Bourgogne, 6 Boulevard Gabriel, Dijon F-21000, France, [§]IsoTis, NV, 10 Prof. Bronkhorstlaan, Gebouw D., Bilthoven 3723 MB, The Netherlands, ^{||}Sylvius Laboratories, Leiden University, Leiden 2300 RA, The Netherlands, ^{**}UMR CNRS/Université Paris-Sud 8621, Institut de Génétique Moléculaire, Equipe BMGE, Orsay Cedex F-91405, France, ^{††}UMR INRA 692 "Biochimie des Interactions Cellulaires," ENESAD, 26 Boulevard du Dr. Petitjean, F-21079 Dijon cedex, France, and ^{§§}Leiden Institute of Chemistry, Gorlaeus Laboratories, Leiden University, 55 Einsteinweg, P.O. Box 9502, Leiden 2300 RA, The Netherlands

We used the combination of preparative electrophoresis and immunological detection to isolate two new proteins from the shell calcitic prisms of *Pinna nobilis*, the Mediterranean fan mussel. The amino acid composition of these proteins was determined. Both proteins are soluble, intracrystalline, and acidic. The 38-kDa protein is glycosylated; the 17-kDa one is not. Ala, Asx, Thr, and Pro represent the dominant residues of the 38-kDa protein, named calprismin. An N-terminal sequence was obtained from calprismin. This sequence, which comprises a pattern of 4 cysteine residues, is not related to any known protein. The second protein, named caspartin, exhibits an unusual amino acid composition, since Asx constitutes by far the main amino acid residue. Preliminary sequencing surprisingly suggests that the first 75 N-terminal residues are all Asp. Caspartin self-aggregates spontaneously into multimers. *In vitro* tests show that it inhibits the precipitation of calcium carbonate. Furthermore, it strongly interferes with the growth of calcite crystals. A polyclonal antiserum raised against caspartin was used to localize this protein in the shell by immunogold. The immunolocalization demonstrates that caspartin is distributed within the prisms and makes a continuous film at the interface between the prisms and the surrounding insoluble sheets. Our finding emphasizes the prominent role of aspartic acid-rich proteins for the building of calcitic prisms among molluscs.

The secretion of a shell by molluscs is a striking example of a self-assembling process performed outside living tissues. When a mollusc builds its shell, the calcifying epithelium of its mantle extrudes mineral ions, mainly calcium and bicarbonate. In addition, it secretes an extracellular matrix composed of proteins, glycoproteins, proteoglycans, and polysaccharides (1). This mixture is released into the extrapallial space, a microvolume delimited by the epithelium, the growing shell, and the

leathery periostracum (2). In this supersaturated space, the released macromolecules interact with bicarbonate and calcium to form biocrystallites that self-aggregate in an orderly manner. The end product is a densely packed organomineral assembly, the shell, in which the mineral phase represents more than 95% by weight (3). As shell proteins exert a control on the biomineralization process, they can be used in the synthesis of biomimetic materials (4–6). However, the resolution of the primary structure of molluscan shell proteins has been seriously impaired for decades by their polydispersity, their polyanionic properties, and finally their post-translational modifications (3, 7).

Despite these obstacles, investigations on molluscan shell proteins have made significant advances in the last 6 years, with the characterization of 16 proteins and, for most of them, the identification of the corresponding transcript (8, 9). Among the different shell textures that molluscs use to produce their shell, mother-of-pearl has received the greatest deal of attention. Its intrinsic beauty, its incredible mechanical toughness (10), and its occurrence in the three major mollusc phyla (11) have indeed contributed to make it the unique model for molluscan mineralization (3, 12). The interest for studying nacre has also been driven by its economical importance in the pearl industry (13) and recently by its promising use for promoting bone repair (14, 15). As a consequence, most of the molecular information accumulated at present concerns nacre proteins.

In contrast, the prismatic texture, that always forms the outer calcified layer of nacreous molluscs, has been studied far less. To our knowledge, only four proteins, including MSI31 and the newly discovered prismalin, aspein, and asprich, have been genetically characterized (16–19). Of these proteins, only prismalin has been characterized both biochemically and at the transcriptional level, the three other protein sequences being simply deduced from their transcripts. Despite the paucity of molecular data, prismatic biominerals fully deserve attention, because they are widespread among molluscs and because prism-like biominerals are also found in other calcifying systems, such as the eggshell (20) and the secondary layer of brachiopods (21). Thus, prism-like biominerals are often considered to represent an efficient and simple strategy adopted by calcifying metazoans for rapid mineralization. Also, because this layer is believed to represent an archaic type of texture, analysis of the associated matrix components may shed light on the molecular mechanisms of early biomineralization (22, 23). Finally, because prisms are large crystals, they represent a good model for studying how molluscs are able to control their mineralization over nanometer to millimeter scales.

Like several Pteriomorphid bivalves, *Pinna nobilis*, the giant Mediterranean fan mussel, exhibits a nacropismatic organization of its shell.

* This work was supported by the "Fondation Simone et Cino Del Duca" (Paris), for the period November 1999 to January 2001, and by the Dutch biotech company IsoTis, for the period February 2001 to December 2002. This paper is a contribution to an "Aide Concertée Incitative Jeunes Chercheurs" (ACI JC 3049) awarded to F. Marin by the French "Ministère Délégué à la Recherche et aux Nouvelles Technologies." In 2004, the "Conseil Régional de Bourgogne" (Dijon, France) provided financial support for the installation of a biomineralization laboratory in Biogéosciences research unit. The costs of publication of this article were defrayed in part by the payment of page charges. This article must therefore be hereby marked "advertisement" in accordance with 18 U.S.C. Section 1734 solely to indicate this fact.

The N-terminal protein sequence of calprismin reported in this paper has been registered in the Swiss-Prot and TrEMBL knowledgebase under the accession number P83631.

¹ To whom correspondence should be addressed: UMR CNRS 5561 "BIOGÉOSCIENCES," Université de Bourgogne, 6 Bd. Gabriel, 21000 DIJON, France. Tel.: 33-3-80-39-63-72; Fax: 33-3-80-39-63-87; E-mail: frederic.marin@u-bourgogne.fr.

Characterization of Two Shell Proteins from Calcitic Prisms

Whereas the nacreous layer is restricted to the first half of the shell, the prismatic layer is fully developed and constitutes the predominant shell layer of this species. It is made of long needles of calcite with a polygonal cross-section. The prisms of *Pinna* represent the so-called "regular simple prism" type (11, 24, 25). Among adult specimens, these prisms can be several mm long with a diameter less than 100 μm . Growing inward from the periostracum (2, 25), they are kept together by an interprismatic organic honeycomb-like framework, which can be destroyed by sodium hypochlorite (26). Optically, each isolated prism behaves as a monocrystal (27). However, despite this apparent simplicity, the calcitic prisms of *P. nobilis* are indeed composed of a stack of numerous crystallites, which have a single optical orientation maintained throughout the length of the prisms. When decalcified, the isolated prisms release a soluble acidic matrix. This matrix is thought to be responsible for the choice of the calcite polymorph and for the guidance and correct positioning of the single crystallites, so that the monocrystal-like units emerge (27). But this matrix has been poorly characterized (26, 28), and recent data acquired on the bulk matrix (29, 30) do not give any information on the molecular mechanisms by which prisms are built. The work described herein aims to elucidate the structure of this acidic macromolecular assemblage. The results of this study represent a biochemical characterization of two so-called "intracrystalline" proteins, which we have named caspartin and calprismis. In addition, this report presents the localization of one of these proteins, caspartin, by combining immunogold labeling and scanning electron microscopy. Finally, this report describes the dramatic effect of this protein on the morphology of calcium carbonate crystals grown *in vitro*.

EXPERIMENTAL PROCEDURES

Shell Material—The species used in this study is the protected Mediterranean fan mussel *P. nobilis* (31). Fragments of shells of juvenile and adult specimens were kindly provided by CERAM (Prof. Nardo Vicente) (Marseille, France). Detailed descriptions of the nacropismatic texture of the shell have been reported (11, 24–26). For direct microscopic observations, cleaned shell fragments or isolated prisms were gold-sputtered with a sputter coater (model 108 Auto; Cressington) and directly observed with a Philips XL30 ESEM-FEG scanning electron microscope (Fig. 1).

Shell Preparation and Matrix Extraction—The shell fragments were scrupulously brushed to remove epibionts, and the nacreous layer, when present, was removed by abrasion. Only the prismatic layer was used for subsequent analysis. Fragments of this layer were soaked in sodium hypochlorite solution (0.2 g of active chlorine/100 ml of water) for 12 h, rinsed with water, and dried.

Cleaned pieces were briefly crushed into minute fragments, which were subsequently treated with dilute sodium hypochlorite (0.2 g of active chlorine/100 ml of water) for 4 days with constant stirring. This treatment resulted in the complete dissociation of the fragments into prisms, which were collected on a membrane by filtering the suspension (Nalgene filtration assembly). The prisms were then extensively rinsed with Milli-Q water and dried before being crushed.

For extraction of the soluble matrix, different batches were used, comprising juvenile or adult specimens. Between 3 and 25 g of the prism powder were suspended in water, to which cold acetic acid (5%, v/v) was added until the pH was 4. Decalcification was performed overnight at 4 °C. The solution was centrifuged for 10 min at 5000 \times g, and the residual insoluble organic matrix was discarded. The clear supernatant was filtered (0.45 μm), and the volume was reduced to approximately 5 ml by ultrafiltration on an Amicon membrane (YM10; cut-off of 10 kDa)

at 4 °C. Complete desalting of the solution was accomplished by dialysis against water at 4 °C for 5 days (Slide-A-Lyzer cassette; Pierce). For some of the batches, this solution was freeze-dried, and the resulting pellet was weighed.

Soluble Matrix Analysis on SDS-PAGE and on Immunoblots—For each batch, the solution containing the concentrated acetic acid-soluble matrix was diluted with an equal volume of 2 \times Laemmli sample buffer containing β -mercaptoethanol. After heat denaturation (32), small aliquots were tested on 10, 12, or 15% discontinuous polyacrylamide SDS-polyacrylamide gels (Mini-Protean 3; Bio-Rad). Most of the gels were directly stained with silver nitrate (33). Other gels were blotted onto PVDF² Immobilon-P membrane (Millipore Corp.) with the Mini-Trans Blot module (Bio-Rad) for 90 min at 120 mA (34, 35). The blots were blocked with 1% gelatin in Tris-buffered saline (TBS) for 30 min and then incubated for 90 min with polyclonal antibodies raised against unfractionated acetic acid-soluble prism and nacre matrices of *P. nobilis* (28). After washing with TBS/Tween 20, the membranes were incubated with a goat anti-rabbit, peroxidase-conjugated antibody (A6154; Sigma) for 90 min. After extensive washing, the membranes were incubated with luminase buffer for 2 min (36) and then briefly exposed to X-Omat film (Eastman Kodak Co.).

Large Scale Matrix Fractionation—For each batch, large aliquots of the denatured matrix were fractionated on a preparative SDS-12% polyacrylamide gel (model 491 Prep Cell, 28-mm tube diameter; Bio-Rad) (37, 38). The gel was run at 250 V for 1 h and then at 300 V overnight in a buffer containing Tris (25 mM), glycine (192 mM), and SDS (0.1%), pH 8.3. The same buffer without SDS was used for eluting protein fractions from the gel. After the elution of the migration front, 80 fractions of 5 ml each were continuously collected overnight (Bio-Rad fraction collector 2110) at a flow rate of 0.5 ml/min.

Since none of the fractions absorbed UV at 280 nm, an immunological detection of the matrix fractions was performed with the anti-prism and nacre matrix antisera (28, 37). Aliquots (100 μl each) of the 80 fractions were vacuum-blotted on a PVDF membrane with a dot blot apparatus (Bio-Rad Bio-Dot). The membrane was subsequently treated like a normal Western blot as described above. Following the result of the dot blot, the tubes containing two identified fractions were pooled and concentrated to 4–5 ml by ultrafiltration (Amicon ultrafiltration cell, cut-off of 10 kDa) before being dialyzed for 5 days against Milli-Q water at 4 °C to remove Tris and glycine. The fractions were freeze-dried. The purity of the two fractions was assessed on a mini-SDS-polyacrylamide gel, which was subsequently stained with silver. Two strong bands of 17 and 38 kDa were observed.

Amino Acid Composition and N-terminal Sequencing—The amino acid compositions of the two fractions were determined by Eurosequence bv, Groningen. Freeze-dried proteins were hydrolyzed with 5.7 N HCl in the gas phase for 1.5 h at 150 °C. The analysis of the hydrolysates was performed on an HP 1090 Aminoquant (39) by an automated two-step precolumn derivatization with *o*-phthalaldehyde for primary and FMOC (*N*-(9-fluorenyl)methoxycarbonyl) for secondary amino acids. Cysteine residues were quantified after pyridylethylation. Tryptophan was not determined. In order to ensure that the samples were not contaminated with free amino acids, in particular glycine, amino acid analyses were also performed without prior hydrolysis.

The N-terminal sequencing was performed with a Hewlett-Packard G1006A Protein Sequencer connected in line to a Hewlett-Packard model 1100 high pressure liquid chromatograph. Edman degradation

² The abbreviations used are: PVDF, polyvinylidene difluoride; TBS, Tris-buffered saline; PTH, phenylthiohydantoin; BSA, bovine serum albumin; TFMS, trifluoromethanesulfonic.

used the Routine 3.1 program, and the sequencing cartridge and most chemicals were obtained from Hewlett-Packard. Ethyl acetate was analyzed by Baker Ultraresi, to which 2.5 μl of tributylphosphine were added per 125 ml. The addition of tributylphosphine substantially improved the yield of the PTH-derivative, especially of lysine.³ During sequencing of calprism, we observed the appearance of an abnormal PTH-derivative in cycles 12, 19, 33, and 40, between PTH-Gly and PTH-His. It is the position of the PTH-derivative of carboxamidoethylcysteine, which may have formed from acrylamide monomer and reduced cysteine during the preparative acrylamide electrophoresis step (see "Large Scale Matrix Fractionation").

Calcium-binding Assay—The calcium-binding capacity of the acetic acid-soluble matrix and of the two purified proteins was analyzed according to two methods: staining with carbocyanine "Stains-All" dye (40) and the overlay method with ⁴⁵Ca (41). In the first case, minigels were run, extensively washed with 25% isopropyl alcohol, and stained in the dark for 4 days with 0.0025% Stains-All, 25% isopropyl alcohol, 7.5% formamide, and 30 mM Tris base, pH 8.8. In the second case, denaturing gels were blotted onto PVDF membranes, which were subsequently soaked three times for 20 min each in an overlay buffer (10 mM imidazole-HCl, pH 6.8, 60 mM KCl, 5 mM MgCl₂) and then incubated in the same buffer containing ⁴⁵CaCl₂ (37 MBq/liter, 1.36 $\times 10^{-3}$ mM). After a brief washing (50% ethanol, twice for 2 min each), the membranes were dried at room temperature and exposed to an x-ray film for 1 week or more. Calmodulin, a calcium-binding protein (catalog number P2277; Sigma), was used as a positive control. To test the effect of Laemmli buffer on the calcium-binding ability of the samples, additional tests were performed. Similar amounts of Laemmli-denatured and nondenatured extracts of soluble matrix and of the 17- and 38-kDa proteins were dot-blotted on a PVDF membrane with a Bio-Dot module (Bio-Rad). The membrane was treated with ⁴⁵Ca as described above. The test was repeated several times.

Glycosylation and Deglycosylation Studies—The search for putative glycosylations of the acetic acid-soluble matrix and of the two isolated proteins was performed according to three different sets of techniques: (a) gel and blot staining, (b) deglycosylation studies, (c) monosaccharide analysis. The first set included staining of the gels with Alcian Blue 8 GX according to the protocol of Wall and Gyi (42) and staining of gels and of Western blots with PAS (43). Deglycosylation studies were performed according to two procedures: chemical deglycosylation with trimethanesulfonic (TFMS) acid/anisole (44) and enzymatic deglycosylation. In the first case, the removal of sugars was performed at 0 °C for 3 h, under N₂, with constant stirring. After neutralization with pyridine, the aqueous phase was extracted three times with diethyl ether and then extensively dialyzed before being lyophilized. In the second case, samples were deglycosylated enzymatically at 37 °C for 3 h, with a mixture containing peptide-N-glycosidase F, O-glycosidase, sialidase, β -galactosidase, and glucosaminidase (CarboRelease Kit, catalog number KE-DG01; QA-Bio, San Mateo, CA). In both cases, fetuin was used as a positive control, and BSA was used as a negative control for the chemical deglycosylation. The TFMS acid-treated and enzyme-treated samples were tested on mini-SDS-PAGE, (10, 12, or 15% acrylamide), which were subsequently stained with silver or blotted on PVDF membranes. The blots were then incubated with the anti-nacre matrix antibody (28). Furthermore, Alcian Blue staining was assayed on the 38-kDa protein, before and after enzymatic deglycosylation. At last, the soluble matrix and the two purified proteins were assayed for monosaccharides (45) before and after hydrolysis. Lyophilized samples (400–800 μg) were

dissolved in water at 1 $\mu\text{g}/\mu\text{l}$. Aliquots of 100 μl were hydrolyzed in 100 μl of trifluoroacetic acid (4N) at 105 °C for 4 h. Samples were evaporated to dryness before being solubilized with 100 μl of 20 mM NaOH. The neutral and amino sugar contents of the hydrolysates were determined by high performance anion exchange-pulsed amperometric detection (Dionex) (46) on a CarboPac PA100 column (Dionex P/N 043055). Data were collected and processed using Chromeleon software (version 6.40). Nonhydrolyzed samples were analyzed similarly, in order to detect free monosaccharides. Blank experiments were performed, where acetic acid solutions had gone through all of the steps of the extraction procedure, to assess possible sugar contamination via filtration and ultrafiltration membranes and dialysis tubing. Note that this technique does not allow the quantification of sialic acids, which are destroyed during hydrolysis with trifluoroacetic acid.

In Vitro Inhibition Test with the 17-kDa Protein—The 17-kDa protein was subsequently assayed for *in vitro* inhibition of calcium carbonate precipitation (47). Two ml of 20 mM CaCl₂ were rapidly added to 2 ml of 20 mM NaHCO₃ containing variable amounts of protein extract (1–10 μg). For each experiment, the pH was constantly recorded with a combined glass electrode (catalog number 6.0234.100; Metrohm) coupled with a Metrohm model 692 pH meter. Each concentration was tested in triplicate. Between each experiment, the electrode was refreshed with 0.5 M HCl. Blank tests were performed in the absence of protein. Positive controls were performed with poly-L-aspartic acid (P-6762; Sigma) and negative controls with BSA.

Growth of Calcite Crystals in the Presence of the 17-kDa Protein—The effect of the 17-kDa protein on the morphology of calcite crystals was tested *in vitro*. Calcite crystals were grown by slow diffusion of ammonium bicarbonate vapors into a CaCl₂ solution (48). Plastic tips were UV-glued on HCl-cleaned microscope glass coverslips (18 \times 18 mm) to allow easy handling with forceps. The coverslips were placed into the wells of a Sterilin 5 \times 5 square-well plate (catalog number 638161; Greiner), to which were added 4 ml of 10 mM calcium chloride containing increasing amounts of the shell protein (0.1–4 $\mu\text{g}/\text{ml}$). Negative controls were performed with similar amounts of bovine serum albumin. Blanks were performed without any protein. The plate was closed with a plastic cover, which had been pierced with 1-mm holes, and then incubated overnight at 4 °C in a closed dessicator containing crystals of ammonium bicarbonate. After incubation, the coverslips were gently dried by capillarity and then by incubation at 50 °C. They were subsequently gold-sputtered and observed with a Philips XL30 ESEM-FEG scanning electron microscope. This test was performed five times.

Polyclonal Antibodies against the 17-kDa Protein—An aliquot of the 17-kDa protein was used for the production of polyclonal antibodies in a rabbit (Eurogentec). A standard immunization procedure was performed with injections at 0, 14, 28, and 56 days and bleedings at 0 (preimmune), 38, 66, and 80 days. Sera (second and third bleeding) containing the polyclonal antibodies were used for subsequent experiments. Their respective titer was determined by standard enzyme-linked immunosorbent assay (49). The specificity of the antiserum for the low molecular weight protein was checked by Western blots on complete acetic acid-soluble prism matrix of *P. nobilis*. The antiserum was also tested on Western blots against the isolated protein, without or after reduction with β -mercaptoethanol. In addition, the antiserum was tested against poly-L-aspartic acid (P-6762; Sigma) and against the acetic acid-soluble matrix extracted from the nacreous shell layer of *P. nobilis*. In this latter case, the nacre matrix was extracted with cold dilute acetic acid, in the same way as the prism matrix.

The same antiserum was used for determining the concentration of the low molecular weight protein in EDTA extracts of the prisms and of

³ R. Amons, unpublished results.

Characterization of Two Shell Proteins from Calcitic Prisms

the nacre matrix of *P. nobilis*. Aliquots of 300 mg of cleaned prisms and of nacre powders were dissolved overnight in 10 ml of 20% (w/v) EDTA. The solutions were centrifuged and filtered, and the supernatants were

serially diluted with EDTA and then vacuum-blotted onto a PVDF membrane. Known amounts (100 pg to 100 ng of the 17-kDa protein) were used as a standard. The membrane was incubated with the antiserum and then treated as a normal blot. The test was repeated four times in triplicate. To check the effect of sodium hypochlorite (used for isolating the prisms) on the degradation of the 17-kDa protein, a control experiment was performed where prism matrices were extracted from sodium bleach-isolated prisms and from untreated prismatic layer and then dot-blotted and treated with the antiserum.

Immunolocalization of the 17-kDa Protein with Gold Particles—The antiserum preparations were used for localizing the 17-kDa protein directly in the shell. Freshly broken pieces of cleaned prismatic layer or isolated prisms were slightly etched with EDTA (1%) for 2 min before being blocked with a 2% gelatin solution in TBS, pH 7.5. As an alternative, polished sections were bleached with sodium hypochlorite for a few minutes and then rinsed with water, etched with EDTA, and blocked with gelatin. The preparations were subsequently incubated for 2 h with the antiserum (second bleeding) diluted 1:3000 in a solution of 2% gelatin in TBS-Tween 20 (TBS-T). After extensive rinsing with TBS-T, the preparations were incubated for 2 h with a similar gelatin-TBS-T solution containing the diluted (1:400) goat anti-rabbit antibody coupled to 5-nm gold particles (catalogue number EM.GAR5; British Biocell International). After extensive rinsing with TBS-T, the preparations were gently dried by capillarity and silver-enhanced for 5–10 min (catalogue number SEKL15; British Biocell International). Blank experiments were performed similarly without the first antibody step or with preimmune serum. The samples were observed with a Philips XL30 ESEM-FEG scanning electron microscope (IsoTis; Biltoven) in the back scattering electron mode. Additional observations were performed with a JEOL JSM 6400F scanning electron microscope (Laboratoire de Réactivité des Solides, Dijon, France).

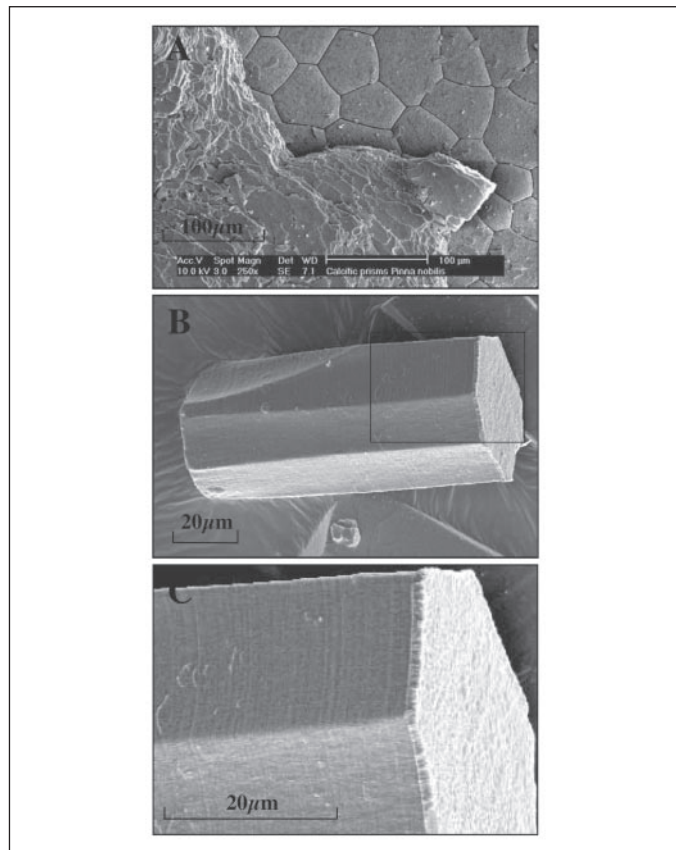


FIGURE 1. Prismatic texture of *P. nobilis* shell. *A*, internal view of the contact between the nacreous (*left*) and the prismatic (*right*) layers of the shell. The sample was cleaned with bleach. The prismatic layer is composed of packed polygonal crystallites, the prisms. *B*, bleach-isolated calcitic prism. *C*, enlarged view of *B*. Although the prisms look homogeneous, a thin layering perpendicular to the long axis of the prisms is visible (*C*). The acetic acid-soluble matrix was extracted from the isolated prisms.

RESULTS

Extraction of Matrix and Characterization on SDS-PAGE—In the present study, we have extracted an acetic acid-soluble matrix from the calcitic prisms of the outer layer of *P. nobilis*. Because the single prisms are isolated with sodium hypochlorite (Fig. 1), this matrix should be

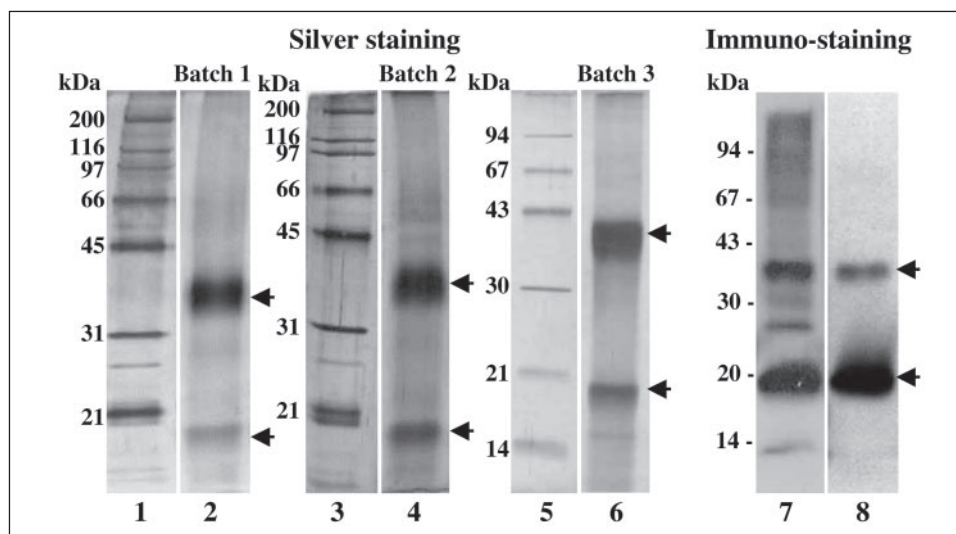


FIGURE 2. SDS-PAGE and Western blot of the acetic acid-soluble prism matrix of *P. nobilis*. The gels were stained with silver, and the blots were probed with polyclonal antibodies (see Ref. 28) raised against the whole acetic acid-soluble matrix extracted from prisms (*lane 7*) and from nacre (*lane 8*). The arrows indicate the position of the two major proteinaceous components of the matrix. Similar amounts of shell matrices were analyzed (20 μ g/lane). Batch 1 and 2 (*lanes 2 and 4*) were matrix from two specimens, aged 2 years. Batch 3 (*lane 6* and *Western blot*) was matrix from 1-year-old specimen. The samples from batches 1 and 2 were run on 12% polyacrylamide gels, and the one from batch 3 was run on a 15% polyacrylamide gel. The two proteins fractionated from batch 3 were used for amino acid composition and for N-terminal sequencing (see Fig. 3). *Lanes 1 and 3*, broad range molecular weight standards. *Lane 5*, low molecular weight standards.

considered as intracrystalline. From the different batches used for this study, the acetic acid-soluble matrix represents 0.26–0.29% by weight of the dry isolated prisms. These values are consistent with previous findings (50, 51). By comparison, the acetic acid-soluble matrix extracted from the nacreous layer of *P. nobilis* represents only 0.02% of the dry nacre (52).

When run on mini-SDS-PAGE and stained with silver (Fig. 2), acetic acid-soluble matrices of the different batches give similar patterns, characterized by the presence of two prominent bands with apparent molecular masses of 17 and 38 kDa. In addition, minor bands are visible in the upper part of the gels and below the 17-kDa protein. The nondiscrete macromolecules, which migrate as a smear, represent a significant component of the matrix from less than 10 kDa to the top of the gel. In comparison with standard proteins, the prism matrix does not stain well with silver. In batch 2, we observe a negative staining in a zone between the two main bands (Fig. 2, lane 4). A negative staining has often been reported for extremely acidic proteins associated with biominerals (53). Coomassie Blue is ineffective to stain the matrix proteins; only the 17-kDa band gives a faint staining (not shown).

From batch to batch, we observe that the upper band has a tendency to broaden, which makes it more difficult to purify. The broadening occurs especially with batches of adult specimens. This suggests that this protein may degrade rapidly *in vitro* or that it cross-links with other components of the biomineral after synthesis. The most discrete band is observed with 3 g of prisms from a very young specimen (Fig. 2, batch 3, lane 6). This batch was used for the amino acid composition and for the N-terminal sequencing. From batch to batch, the low molecular weight protein appears to be stable. Thus, it has been extracted in larger amounts and further characterized.

On Western blots stained with antisera raised against unfractionated matrix (anti-prism and anti-nacre matrices, respectively), the pattern is clearer than the one obtained after silver staining (Fig. 2, lanes 7 and 8). Since the two main bands are very immunogenic, they give a strong signal. Two additional bands, which are not visible on silver-stained gels, can be detected between 17 and 38 kDa (lane 7). The Western blot pattern has allowed us to perform a large scale fractionation of the matrix by preparative electrophoresis and to purify the two main discrete polypeptides (37, 38). From batch 3, we have extracted less than 200 μ g of the 38-kDa protein, whereas more than 8 mg of the 17-kDa protein have been obtained from the three batches. When tested again on a minigel in denaturing conditions, the two bands appear as single bands (Fig. 3).

Amino Acid Composition and Sequence Analysis—Fig. 3 indicates the amino acid composition of the unfractionated acetic acid-soluble matrix and of the two isolated proteinaceous bands. All three compositions are acidic. The composition of the soluble matrix is characterized by an extremely high amount of Asx, which represents almost two-thirds of the residues. This composition is very similar to that of the intraprismatic organic matrix of *Pinna carnea* determined by Nakahara *et al.* (54). The bulk composition also shows similarities to that of the soluble prism matrix of *Atrina rigida* (48, 55). The main difference is the level of Glx residues, which is much higher in the case of *Atrina*. The other amino acid residues that are quantitatively abundant in the bulk soluble matrix are Ala, Glx, and Gly. The composition of the 17-kDa band is similar to that of the whole soluble matrix, with a striking 68% Asx. This suggests that the nonanalyzed polydisperse components of the matrix are also extremely acidic or that the 17-kDa protein is predominant in the soluble matrix. At 8.3%, Glx is another abundant residue. Except Ala and Gly, which represent, respectively, 6 and 5%, all of the other residues are below 2%. Surprisingly, in the first 75 cycles of

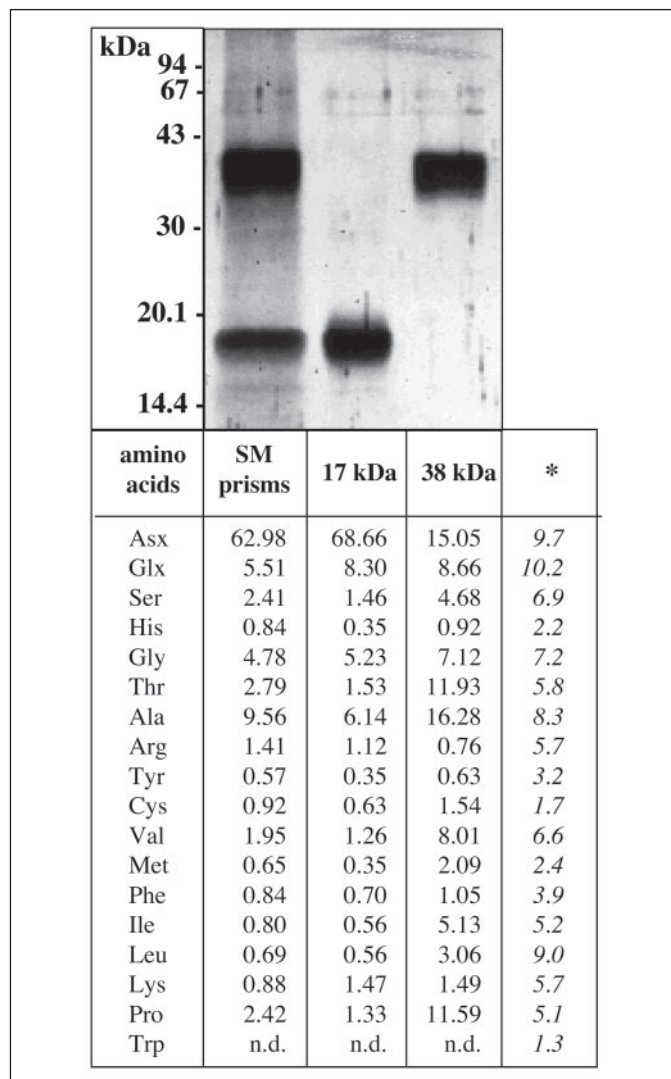


FIGURE 3. Purification and amino acid composition of the acetic acid-soluble prism matrix (SM prisms) and of the 17- and 38-kDa proteins. The two proteins were purified by preparative electrophoresis and analyzed again on mini-SDS-PAGE to assess their purity. The gel was stained with silver. The amino acid compositions of the two proteins were determined and compared with that of the soluble matrix prisms. The data are presented as percentage of total amino acid for each sample. Right column, average occurrence of amino acids determined for a large number of proteins (91).

N-terminal sequence analysis of the 17-kDa protein, only aspartic acid residues are observed. As sequencing proceeded, an increasing part of the protein might have become out of phase. In the absence of the appearance of an amino acid other than Asp, further sequencing beyond cycle 75 was considered useless. Enzymatic cleavages did not allow the determination of internal sequences. Attempts to sequence this protein also revealed that the molecular weight determined by SDS-PAGE may be overestimated.⁴ A crossed search made with AACompIdent (56), combining similarities of amino acid compositions, acidic isoelectric point, and a 0–40-kDa molecular mass range, produced aspolin 2, an acidic fish muscle protein (57), which exhibits 66% Asp residues. On the other hand, a scan for a long polyaspartic acid pattern with ScanProsite (58) yielded chicken calsequestrin and its homolog, aspartactin, and diverse yeast proteins. Calsequestrin is a high capacity, low affinity calcium-binding protein of the endoplasmic reticulum (59), whereas

⁴ R. Amons, personal communication.

Characterization of Two Shell Proteins from Calcitic Prisms

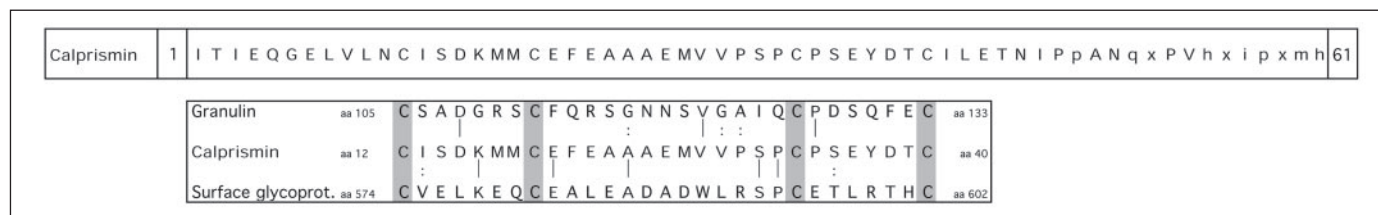


FIGURE 4. N-terminal sequence of calprismin, the 38-kDa protein of the acetic acid-soluble prism matrix. The cysteine pattern (shaded blocks) is aligned with that of vertebrate granulin (Swiss-Prot accession number P28799) and of the major surface glycoprotein of *Pneumocystis carinii*, an ascomycete (Swiss-Prot accession number Q02744).

aspartactin is an extracellular matrix protein (60), which binds laminin. Both contain a long C-terminal poly-Asp domain. Curiously, our ScanProsite search produced neither aspein nor asprich, two newly found shell proteins (18, 19) that exhibit poly-Asp domains.

The overall amino acid composition of the 38-kDa protein is acidic, although less so than the 17-kDa protein and the matrix as a whole (Fig. 3). The 38-kDa protein is dominated by 4 amino acids, Ala, Asx, Thr, and Pro, all above 11% (Fig. 3). Glx, Val, and Gly represent the other abundant residues. The level of serine is low. The high percentage of proline and threonine might suggest that the 38-kDa protein is *O*-glycosylated (61). N-terminal sequencing yielded 61 residues (~18% of the sequence, accession number P83631), of which the first 45 residues are quite certain (Fig. 4). The sequenced portion contains 9 acidic residues, 7 of which are glutamic acid, and only one basic amino acid (Lys¹⁶). The N terminus does not reflect the overall composition of the protein. In particular, 4 cysteine residues are present, separated by 6, 13, and 6 residues, whereas this residue represents only 1.5% of the overall composition. It should be remembered, however, that part of the Cys has already been alkylated to *S*-carboxamidoethylcysteine during acrylamide electrophoresis. A BLAST search (62) does not reveal a clear homology with any protein occurring in the data bases. Some sequence similarities are found with a putative type III effector from *Pseudomonas* (SwissProt accession number Q7PC42). A ScanProsite search for a cysteine signature involving the pattern CX₆CX₁₃CX₆C, with *X* being any amino acid except cysteine, produced more than 100 results, among which are agrins, granulins, and a wide variety of fungal surface glycoproteins. Note that the cysteine pattern of the 38-kDa protein differs from that of other extracellular matrix proteins: the 4-cysteine signature (CX_{2,3}CXCX_{6,9}C) found at the N terminus of small leucine-rich proteoglycans (63, 64) or the cysteine pattern of the cystine knot-containing hormones (65). This pattern is likewise not similar to the cysteine patterns found in other molluscan shell proteins: N16 (66), perlucin (67), and perlustrin (68). A search for post-translational modifications suggests putative phosphorylations of the two serine residues at positions 31 and 35 (69) or, alternatively, one *O*-glycosylation of serine 31 (70). On the other hand, a search made with ScanProsite indicates two putatively phosphorylated serines, at positions 14 and 35. The single Tyr of the sequence, at position 37, is surrounded by two acidic residues (Glu at position 36 and Asp at position 38), a context that favors sulfation (71). Tyrosine sulfation was however not observed by sequencing.⁴

These two proteins appear to be novel, and we have chosen to name the 17- and 38-kDa proteins caspartin and calprismin, respectively.

Calcium-binding Assay—The calcium-binding assays were performed in denaturing conditions on gels (Fig. 5A) and on Western blots (Fig. 5B). The unfractionated soluble matrix stains purple with carbocyanine dye (Fig. 5A, lane 1). Staining of the matrix produces a continuous smear from 10 to 70 kDa. Isolated caspartin and calprismin also stain purple (Fig. 5A, lanes 2 and 3). With the ⁴⁵Ca overlay test (Fig. 5B), the acetic acid-soluble extract of the prisms exhibits a weak calcium binding activity (lane 2), even at high concentration (30 μg/well). A

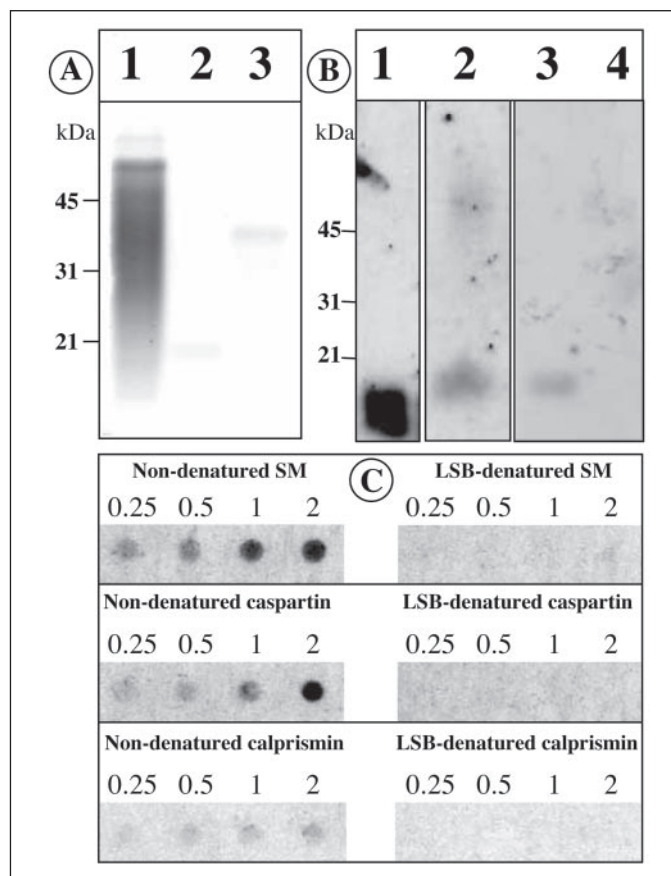


FIGURE 5. Calcium-binding properties of the acetic acid-soluble prism matrix (SM), of caspartin and of calprismin. A, staining with the carbocyanine dye Stains-All. Lane 1, soluble matrix (10 μg); lane 2, caspartin (~5 μg); lane 3, calprismin (~5 μg). B, ⁴⁵Ca-binding overlay test. Lane 1, calmodulin (2 μg); lane 2, soluble matrix (30 μg); lane 3, caspartin (20 μg); lane 4, calprismin (20 μg). C, ⁴⁵Ca-binding overlay test on dot blots of the soluble matrix, of caspartin and of calprismin in denaturing (in the presence of Laemmli sample buffer (LSB)) and nondenaturing conditions. Different amounts were tested (0.25, 0.5, 1, and 2 μg). The soluble matrix exhibits the strongest calcium binding activity, and calprismin exhibits the lowest. Laemmli-treated samples have lost their ability to bind calcium.

diffuse signal is detected at molecular masses above 50 kDa and also where caspartin is located. Because the macromolecular components above 50 kDa are extremely minor components of the matrix, they may, however, represent a potent calcium binding activity. In our different attempts with purified caspartin and calprismin, we observe that caspartin weakly binds calcium but only when concentrated (Fig. 5B, lane 3, 20 μg/lane). This effect is lost when lower amounts of caspartin are used (data not shown). Calprismin does not bind calcium (Fig. 5B, lane 4). By comparison, calmodulin binds calcium, even at 2 μg/lane (Fig. 5B, lane 1).

The soluble matrix did not migrate properly in the gel under non-denaturing conditions. Consequently, the calcium binding activity of the

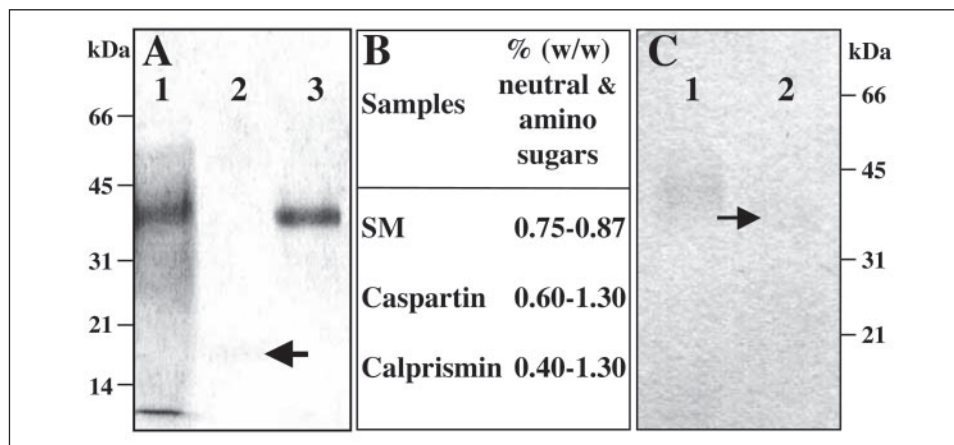


FIGURE 6. **Glycosylation study of the acetic acid-soluble prism matrix (SM), of caspartin, and of calprismin.** *A*, staining with Alcian blue. Lane 1, soluble matrix (20 μg); lane 2, caspartin (10 μg); lane 3, calprismin (10 μg). The soluble matrix and calprismin stain well with Alcian blue, whereas caspartin, localized by the arrow, hardly stains. *B*, determination of the amount of neutral and amino sugars (in percentage of dry weight) after hydrolysis of the samples with trifluoroacetic acid and analysis by high performance anion exchange-pulsed amperometric detection. Batches 1 and 2 were used for the analysis. The three samples are characterized by low amounts of neutral and amino sugars. *C*, staining of calprismin with Alcian blue before (lane 1; 10 μg) and after (lane 2; 10 μg) an enzymatic deglycosylation. A decrease of the staining can be observed after the deglycosylation treatment. The arrow localizes the deglycosylated calprismin.

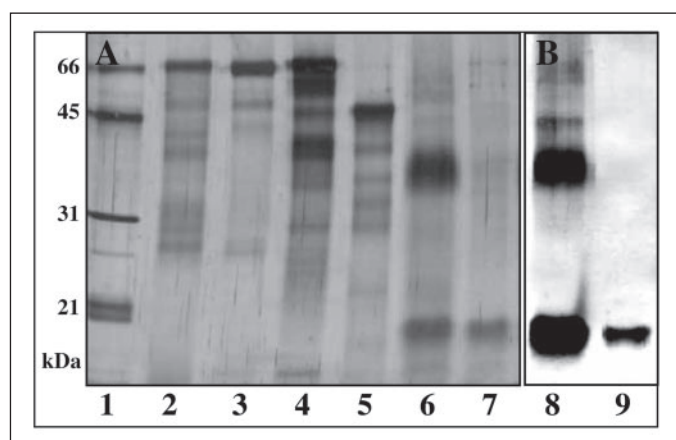


FIGURE 7. **Chemical deglycosylation study with TFMS acid at 0 °C.** Analysis of the samples on silver-stained gel (12% acrylamide (*A*)) and on Western blot (12% acrylamide (*B*)). Lane 1, broad range molecular weight standards; lane 2, nontreated BSA; lane 3, TFMS acid-treated BSA, negative control; lane 4, untreated fetuin; lane 5, TFMS acid-treated fetuin, positive control; lanes 6 and 8, untreated prism soluble matrix (10 μg); lanes 7 and 9, TFMS acid-treated prism soluble matrix (10 μg). The Western blot was incubated with the anti-nacre matrix serum (28). Note that the TFMS acid treatment denatures caspartin epitopes and eliminates the immunological signal for calprismin. This suggests that the TFMS acid treatment degrades calprismin.

soluble matrix and of the two isolated proteins was tested on dot blots under nondenaturing and denaturing conditions. Fig. 5C (left column) shows that the three samples exhibit calcium binding activity when they are solubilized in Tris buffer. The intensities of the signals are, however, different. The soluble matrix exhibits the strongest calcium-binding capacity, which can still be clearly detected at 0.25 μg . Isolated caspartin has a moderate calcium-binding capacity, which tends to drop below 1 μg . Isolated calprismin exhibits a weak calcium binding activity, which slightly decreases from 2 to 0.25 μg . Although the calcium-binding signal is low for calprismin, it is significantly higher than the background signal, obtained with the Laemmli-denatured samples. These results suggest that the calcium binding activity of the soluble matrix is not due entirely to caspartin and calprismin but that other components are involved in this property. This is in agreement with the data obtained with Western blot, which show that macromolecular components above 50 kDa participate in the calcium binding activity of the matrix. In denaturing conditions, the calcium-binding effect of the three prepara-

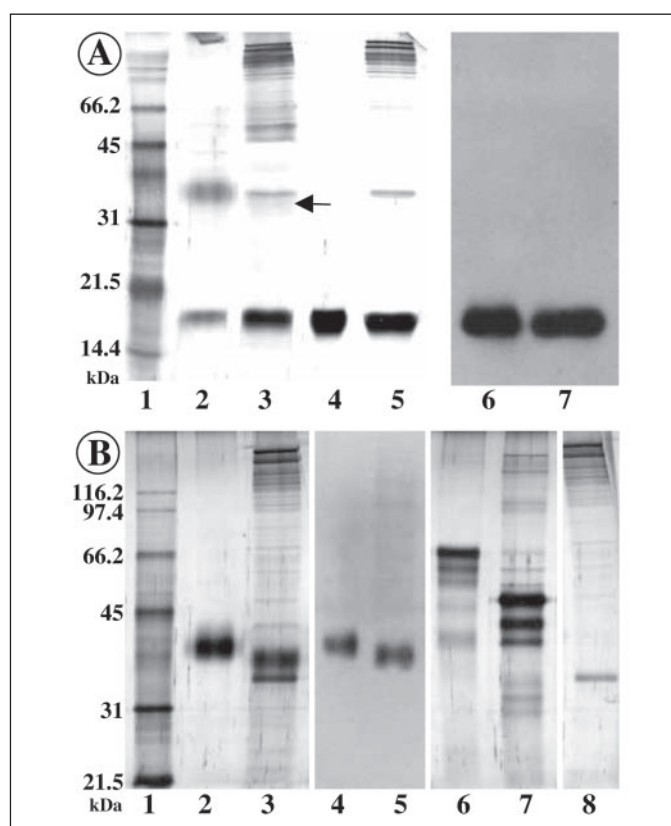
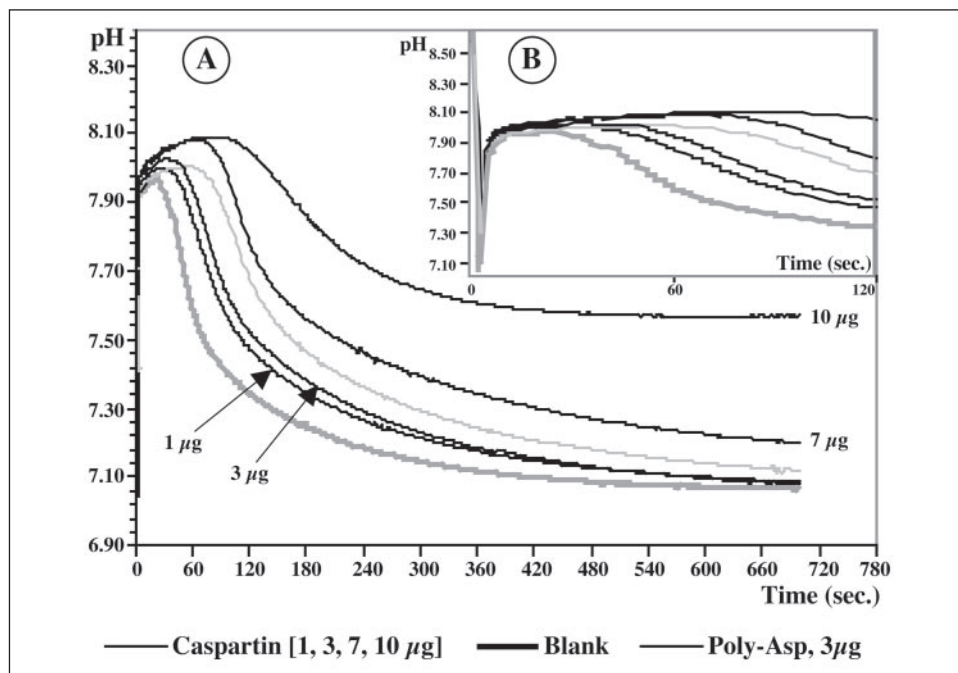


FIGURE 8. **Enzymatic deglycosylation of the soluble matrix, of caspartin, and of calprismin.** A mixture of five enzymes was used. *A*, 15% acrylamide gel stained with silver (lanes 1–5) and Western blot (lanes 6 and 7). Lane 1, broad range molecular weight standards; lane 2, untreated prism soluble matrix (10 μg); lane 3, enzyme-treated prism soluble matrix (10 μg); lanes 4 and 6, untreated caspartin (6 μg); lanes 5 and 7, enzyme-treated caspartin (6 μg). The Western blot was incubated with anti-nacre matrix serum (28). The arrow in lane 3 localizes the deglycosylated calprismin. *B*, 10% acrylamide gel stained with silver (lanes 1–3 and 6–8) and Western blot (lanes 4 and 5). Lane 1, broad range molecular weight standards; lanes 2 and 4, untreated calprismin (5 μg); lanes 3 and 5, enzyme-treated calprismin (5 μg); lane 6, untreated fetuin; lane 7, enzyme-treated fetuin, positive control; lane 8, negative control with the enzyme mixture alone.

tions disappears completely, when tested in the range 0.25–2 μg (Fig. 5B, right column). Weak signals are recorded for higher concentrations (10–20 μg , not shown). This suggests that the affinity of the three tested

Characterization of Two Shell Proteins from Calcitic Prisms

FIGURE 9. *A*, *in vitro* inhibition of the precipitation of CaCO_3 by caspartin, the 17-kDa protein. The graph shows that caspartin starts to be effective at 1 μg . The delay is dose-dependent. *B*, same graph, expanded scale, representing the first 120 s.



samples (soluble matrix, caspartin, calprismin) for calcium is probably low and conformation-dependent.

Glycosylation and Deglycosylation Studies—Fig. 6A shows the results of Alcian blue staining, whereas Fig. 6B indicates the proportion of neutral and amino sugars found in two batches of acetic acid-soluble matrices, caspartin and calprismin. Alcian blue is a cationic dye, which stains mucopolysaccharides and glycosaminoglycans. It is thought to complex with anionic sites of polysaccharides. The acetic acid-soluble matrix appears heavily stained with this dye (Fig. 6A, lane 1). In particular, the most intense staining is observed around 38 kDa, where calprismin is located. A strong staining of isolated calprismin is confirmed in lane 3. On the other hand, caspartin is hardly stained with Alcian blue (lane 2). Different attempts to stain the matrix and the two isolated proteins with PAS (not shown) failed, both on gels and on blots. The absence of staining with PAS is consistent with the extremely low amounts of neutral and amino sugars, determined by high performance anion exchange-pulsed amperometric detection chromatography after acidic hydrolysis, which do not exceed 1.3% (w/w) for the two proteins and are even lower for the whole soluble matrix (Fig. 6B).

To preclude any ambiguities on putative glycosylation of the two proteins, chemical and enzymatic deglycosylations were performed and tested on SDS-PAGE and on Western blots. The results are shown in Fig. 7 for the chemical deglycosylation and in Figs. 8 and 6C for the enzymatic one. After a standard chemical deglycosylation performed at 0 °C, we do not detect any molecular weight shift for caspartin, both on a gel and by Western blot (Fig. 7, lanes 7 and 9), but there is a clear decrease of the immunological signal on the Western blot (lane 9). This indicates, first, that caspartin is apparently not glycosylated and, second, that the treatment with TFMS acid denatures conformation-dependent epitopes of caspartin. Furthermore, the calprismin band completely disappears, both on the silver-stained gel and on the Western blot. This suggests that calprismin may be extremely labile and cannot withstand the harsh treatment. The enzymatic deglycosylation (Fig. 8) confirms the absence of glycosylation of caspartin, since no increase of electrophoretic mobility is observed on a 15% acrylamide gel (Fig. 8A, lanes 5 and 7). Interestingly, on a 10% acrylamide gel, we observe a clear shift of

the calprismin band toward lower molecular weight after the enzymatic deglycosylation, both on the gel and on the blot (Fig. 8B, lanes 3 and 5). A precise calibration with the molecular weight markers indicates that calprismin decreases 2 kDa in apparent molecular mass. Furthermore, we observe a decrease (but not a complete loss) of the staining of calprismin with Alcian blue after the enzymatic deglycosylation (Fig. 6C, lanes 1 and 2). This suggests that the sugars bound to calprismin are negatively charged.

Taken together, our study on glycosyl moieties suggests that calprismin is a true glycoprotein, the saccharides of which are likely to be acidic rather than neutral or aminated. On the other hand, caspartin is not (or is very poorly) glycosylated.

In Vitro Inhibition of Calcium Carbonate Precipitation—Fig. 9 shows the results of the inhibition test. In the blank experiments (no added protein), the pH variations are characteristic. When CaCl_2 is added to the NaHCO_3 solution, the pH decreases instantaneously from 8.5/8.6 to 7.83 before rising again to 8 in ~30 s. Then the pH decreases rapidly to reach pH 7.1 in ~5 min. This pH decrease corresponds to the precipitation of calcium carbonate. The addition of caspartin to the system drastically changes the shape of the curve. One μg is sufficient to induce a delay in the crystallization of calcium carbonate. The delay increases in a dose-dependent manner when 3, 7, and 10 μg are tested. At high amounts (>20 μg), a complete inhibition is recorded (data not shown). A similar effect is observed with poly-L-aspartic acid. By contrast, BSA has no effect on the delay, even at a high concentration (100 μg ; not shown).

Interaction of Caspartin with the Growth of Calcite—Fig. 10 shows the effect of caspartin on the *in vitro* crystallization of calcium carbonate. In a blank experiment without any protein (Fig. 10, A and B), the crystals obtained are rhombohedral with an edge length of ~50 μm . Their surface is smooth. The density of crystals per square millimeter was high, ~70–80. At low concentrations of caspartin (<0.2 $\mu\text{g}/\text{ml}$), we do not observe any effect on the morphology of the crystals.

The effect of caspartin starts to be apparent at concentrations of 0.25–0.5 $\mu\text{g}/\text{ml}$ (Fig. 10C), where a few crystals exhibit morphological changes. At 1 $\mu\text{g}/\text{ml}$ caspartin, the changes affect all of the crystals (Fig.

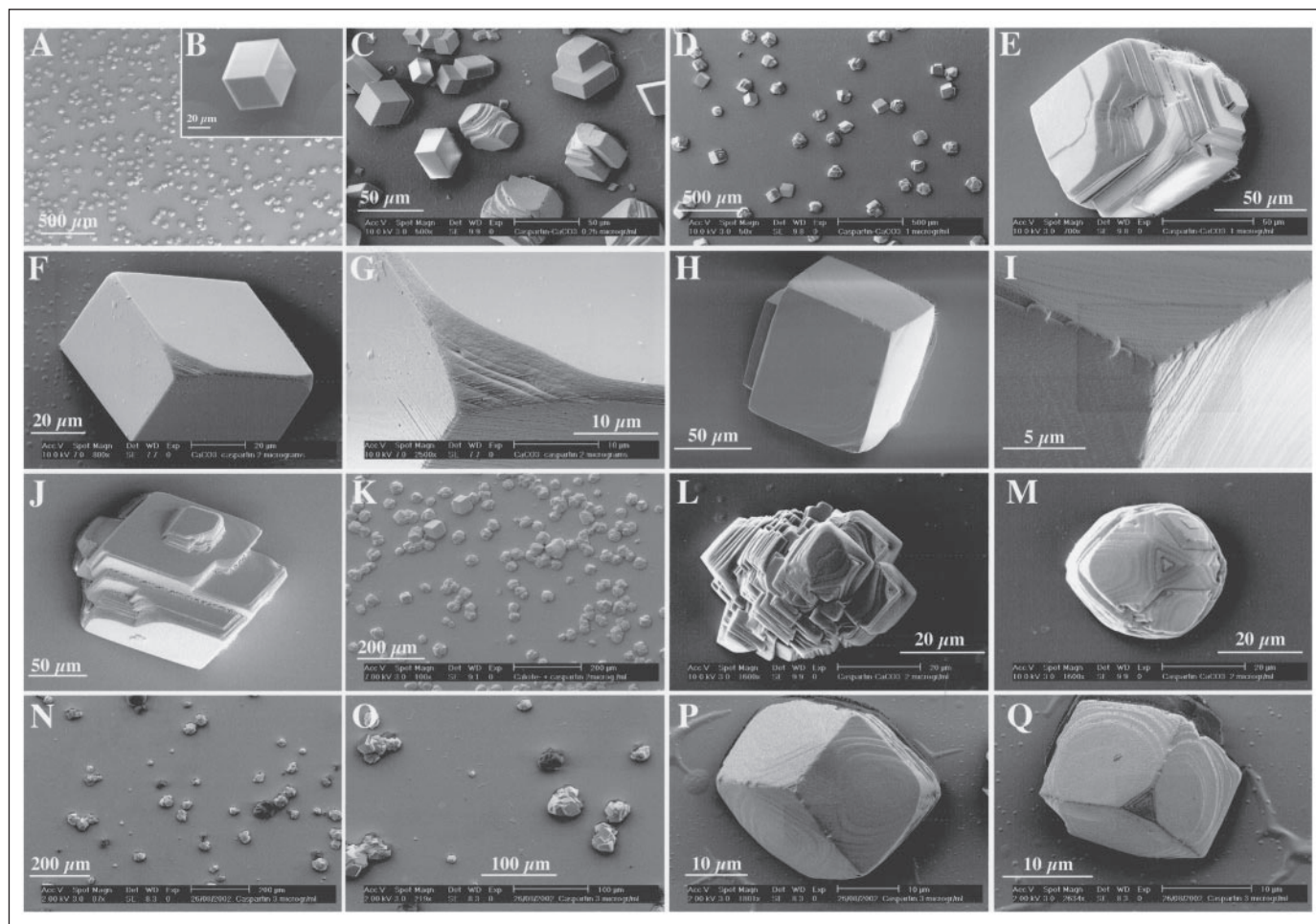


FIGURE 10. *In vitro* crystallization of calcite in the presence of caspartin. Caspartin was tested at concentrations ranging from 0.1 to 5 μg per ml of CaCl_2 solution. A and B, negative control without caspartin. C, caspartin at 0.25 $\mu\text{g}/\text{ml}$. D–J, caspartin at 1 $\mu\text{g}/\text{ml}$. K–M, caspartin at 2 $\mu\text{g}/\text{ml}$. N–Q, caspartin at 3 $\mu\text{g}/\text{ml}$. Above 3 $\mu\text{g}/\text{ml}$, no crystals were formed.

10, D–J). At low magnification, we observe a drastic drop of the density of crystals per surface unit, between 5 and 10 crystals/ mm^2 (Fig. 10D). The crystals obtained are much bigger than those formed in the absence of caspartin, with dimensions of 70–100 μm . Size distribution of the crystals is homogeneous. At higher magnification, the change in morphology is obvious, and two crystal morphologies are observed: polycrystalline aggregates (Fig. 10, E and J) and “monocrystals” (Fig. 10, F–I). The polycrystalline aggregates represent the majority of the crystals, and they exhibit complex morphologies. The “monocrystals” exhibit cubic or quadratic shapes characterized by rounded edges. Some of them exhibit surfaces that are not smooth but are characterized by the formation of terraces (Fig. 10H). At higher magnification (Fig. 10I), microsteps are visible, corresponding to the successive layers forming the sides. For this type of crystal, the effect of caspartin seems to be identical for all the sides of the crystals. The second type, present in low abundance, exhibits a layered structure in one dimension (Fig. 10, F and G).

At 2 $\mu\text{g}/\text{ml}$ caspartin, the size distribution of the crystals is heterogeneous. Whereas most of the crystals are smaller than the ones grown at 1 $\mu\text{g}/\text{ml}$ caspartin, few crystals exhibit similar dimensions (Fig. 10K). Most of the crystals are polycrystalline aggregates (Fig. 10, L and M). At 3 $\mu\text{g}/\text{ml}$, the inhibiting effect of caspartin is readily apparent. The density of crystals per unit area is drastically decreased, as is the size of the crystals (Fig. 10, N and O). The bigger crystallites are all polycrystalline aggregates, whereas minute crystals (10–15 μm) are also present. These

minute crystals exhibit regular cubic shapes, the surfaces of which form regular terraces (Fig. 10, P and Q). At higher concentrations of caspartin, no crystals are observed. Controls performed with BSA do not show any of these effects.

To recapitulate, the concentration range in which the effect of caspartin is visible is narrow (0.5–3 $\mu\text{g}/\text{ml}$). Interestingly, a similar concentration range was previously found for an unfractionated shell extract (48).

Polyclonal Antibodies Raised against Caspartin—Extraction of caspartin from different batches yielded more than 8 mg of lyophilized caspartin, of which 1 mg was used to produce polyclonal antibodies in a rabbit. In ELISA, the working dilutions of the antisera obtained (first, second, and third bleedings) were 1:2000, 1:3000, and 1:10,000, respectively. When tested on a complete acetic acid-soluble extract of the prisms (Fig. 11A, lane 2), the antiserum (second bleeding) reacts against caspartin but does not cross-react with any other component of the prism matrix. The specificity of this antiserum allows us to use it for immunolocalizing caspartin within the shell.

We also observe that this antiserum does not cross-react with poly-L-aspartic acid (Fig. 11A, lane 5), although caspartin exhibits a putative poly-Asp domain. Two explanations can be put forward; such a domain is nonimmunogenic, or the caspartin-reactive antibodies are directed against the more hydrophobic part of the protein.

Interestingly, when lyophilized caspartin is dissolved in unheated or heated Laemmli buffer, which does not contain β -mercaptoethanol (Fig. 11, A (lane 4) and C), we observe a regular banding pattern, whereas the

Characterization of Two Shell Proteins from Calcitic Prisms

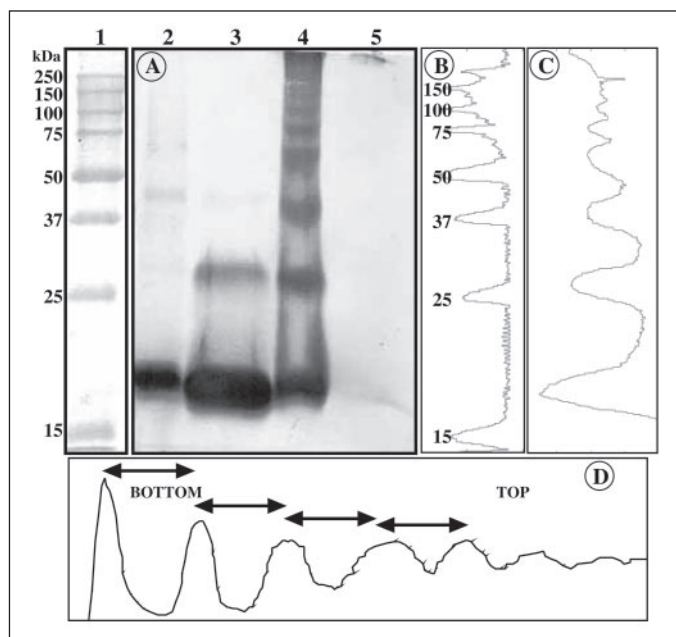


FIGURE 11. Western blot (A) of the prism matrix (lane 2) and of caspartin (lanes 3 and 4) after incubation with the anti-caspartin antibody. The samples were denatured in Laemmli buffer containing (lanes 2, 3, and 5) or not containing (lane 4) β -mercaptoethanol. Lane 1, molecular mass standards (kDa). Lane 5, polyaspartic acid. Densitometric profile of the standards (B) and of caspartin from lane 4 (C). D, densitometric profile of caspartin plotted on a semilog scale. The step (about 13/14 kDa) is conserved from peak to peak. This suggests that caspartin polymerizes in the absence of β -mercaptoethanol.

same preparation heated in a solution containing β -mercaptoethanol produces mainly one band. This suggests that caspartin has the ability to spontaneously self-aggregate into multimers. The densitometric profile, when plotted on a semilog scale (Fig. 11D), shows that the step between neighboring peaks is approximately constant and about 13/14 kDa. On the 12% polyacrylamide gel of Fig. 11, all the oligomers between the dimer and the heptamer can be distinguished. The step value, deduced from a precise calibration of the protein bands on a semilog graph (not shown), is lower than the apparent molecular weight of caspartin. This discrepancy may indicate that the molecular weight of caspartin, deduced from gel electrophoresis in the presence of SDS and β -mercaptoethanol, is overestimated, as previously suspected during our attempts to sequence caspartin. Similar differences in molecular weights have already been observed in many cases. In particular, E7, an acidic protein (pI 4.01), was found to migrate at 17 kDa in denaturing conditions, whereas its true molecular mass was only 11 kDa (72).

The fact that caspartin oligomerizes suggests that it may contain at least two cysteine residues per molecule. Our amino acid analysis (Fig. 3) shows that Cys represents less than 1%, which suggests only one cysteine residue per molecule. This discrepancy may be explained in two ways; the cysteine quantification after pyridylethylation underestimates the amount of this amino acid, or the oligomerization of caspartin may occur by a mechanism different from disulfide bond formation (electrostatic or hydrophobic interactions, van der Waals forces).

Presence of Caspartin in Shell Extracts—The polyclonal anti-caspartin antiserum was tested on dot blots of EDTA extracts of prism and nacre matrices (Fig. 12, A and B). In addition, this antibody was tested on Western blots of the two matrices (Fig. 12C). The results of the dot blots indicate that caspartin is mainly concentrated in the prismatic layer. Although our test is only semiquantitative, we estimate that caspartin represents between 2.4 and 5% of the acetic acid-soluble prism matrix (60–125 μ g of caspartin/g of bleach-treated prism powder). The inten-

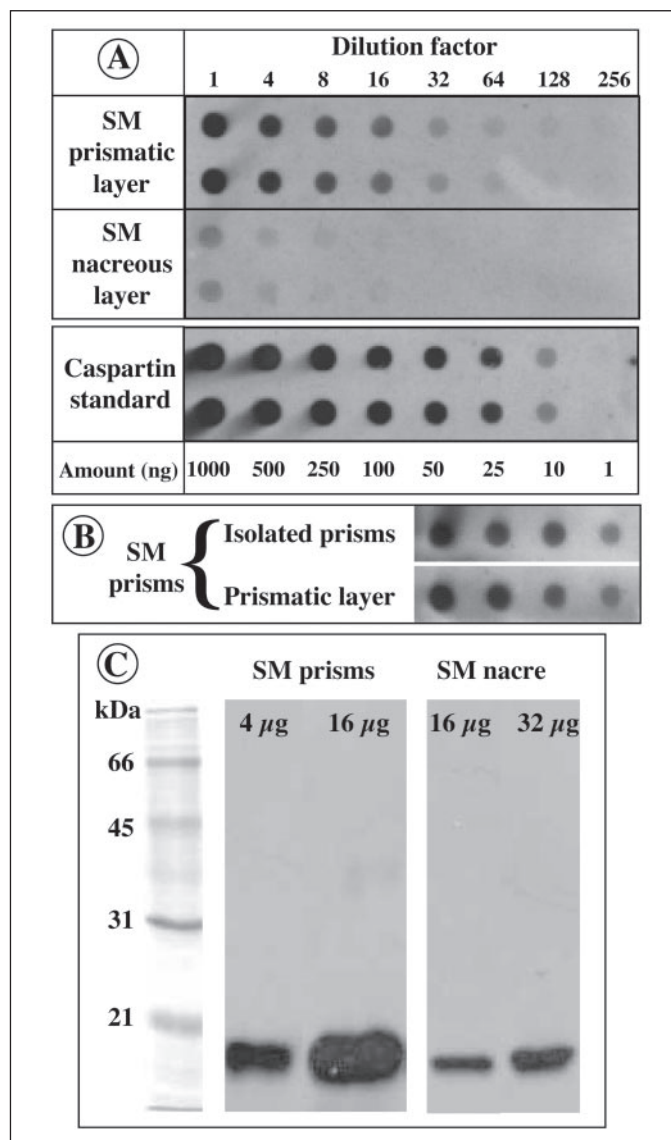


FIGURE 12. Presence of caspartin in prism and nacre EDTA extracts. A, dot blot semi-quantification of caspartin in prism and nacre extracts. The extracts were compared with known amounts of caspartin, which were serially diluted in EDTA. The blot shows that a strong signal is detected in the prism extract and that a weak one is detected in the nacre matrix. B, comparison of the immunological reactivities of the EDTA-soluble matrices extracted from bleach-isolated prisms and from untreated prismatic layer. The reactivities are similar. SM, soluble matrix. C, Western blot of prism and nacre matrices (4, 16, and 32 μ g/lane). The blot was incubated with the anti-caspartin antiserum (dilution 1:5000). Caspartin is present in the soluble matrix of both layers, although in higher concentrations in the prism extract.

sities of the signals obtained from isolated bleach-treated prisms and from pieces of the prismatic layer are not significantly different (Fig. 12B). The slight variations might be due to the removal of insoluble organic periprismatic sheaths, which account for 5% of the weight of the powder. In comparison, the dot blot signal obtained with the nacre EDTA extract is low but significant. An approximate quantification of the amount of caspartin/g of dry powder indicates that caspartin or caspartin-related proteins would be 20–50 times less concentrated in the nacre than in the prisms. To test that the weak signal obtained on the nacre matrix is due to caspartin, or caspartin-related peptide, we also performed Western blots with increased amounts of prisms and nacre matrices. The results, shown in Fig. 12C, indicate that the nacre matrix contains an immunoreactive band, which is located at the same height on the gel as caspartin. However, this band is much less concentrated

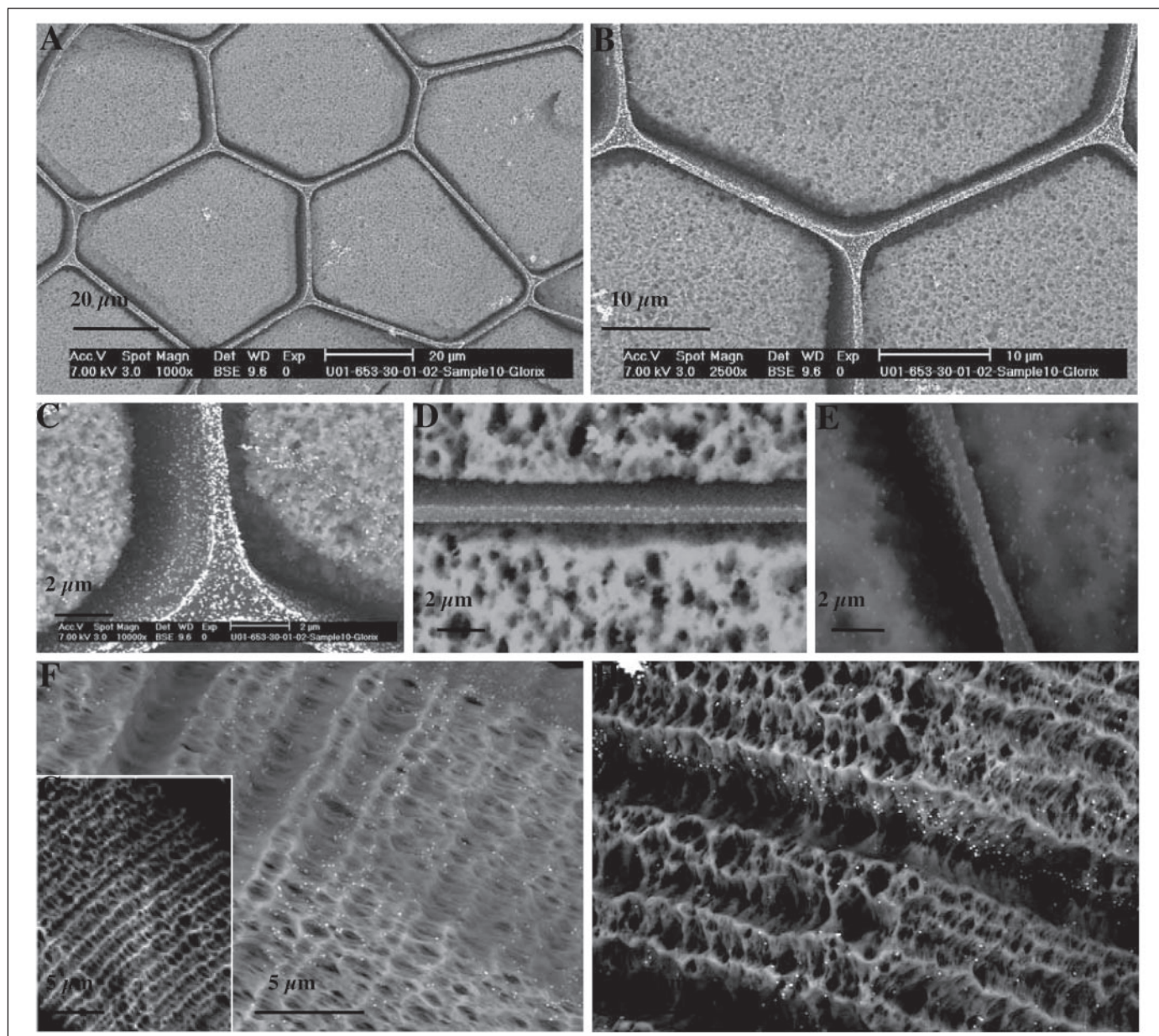


FIGURE 13. **Immunogold localization of caspartin in prisms.** Samples were observed in the back-scattered electron mode. *A–C*, transverse sections. *D* and *E*, longitudinal sections. *F–H*, surfaces of isolated prisms. *A–C* show that caspartin forms a continuous double layer at the interface between the periprismatic insoluble sheaths and the polygonal crystals. In addition, caspartin is dispersed within the crystals. *D* and *E*, a similar distribution of caspartin is observed in longitudinal sections. *F*, caspartin is homogeneously dispersed along the length of the prisms. *H*, in some areas, caspartin is preferentially concentrated in planes, which are perpendicular to the long axis of the prisms. Despite a layering of the prisms (see also Fig. 1), we do not observe any continuous layer of caspartin in that dimension. *G*, negative control with preimmune serum.

than caspartin in the prisms; 4 μg of prism extract gives a signal that is higher than the one obtained with 32 μg of nacre extract. These data suggest that caspartin, although enriched in the prism matrix, is not specific to that layer.

Localization of Caspartin in Shell Preparation by Immunogold—Results of the immunogold staining of caspartin in shell sections and in isolated prism preparations are shown in Fig. 13. In the back-scattered electron mode, the complexes formed by the antigen + first antibody + gold-labeled second antibody are localized as bright spots, the size of which is increased by silver enhancement (100 nm and more). In transverse sections, caspartin is seen as a continuous double layer coating the two sides of the insoluble organic sheaths

that surround the crystals (Fig. 13, *A–C*). At higher magnification, it can be seen that caspartin is also distributed inside the prisms (Fig. 13*C*). On longitudinal sections (Fig. 13, *D* and *E*), the double layer coating the insoluble sheath is also observed as well as scattered bright spots within the prisms (Fig. 13*E*). In the longitudinal view of isolated prism preparations, caspartin is localized on the surface of the prism sides (Fig. 13*F*). It is not clear whether the distribution of caspartin in that dimension is more or less uniform, as Fig. 13*F* suggests, or whether caspartin is preferentially concentrated in certain planes, perpendicular to the axis of the prisms, as shown in Fig. 13*H*. Although the layered structure of isolated prisms is evident, we do not observe continuous layers of caspartin, which would corre-

Characterization of Two Shell Proteins from Calcitic Prisms

spond to these layers. The negative controls produce a low background (Fig. 13G).

DISCUSSION

The new method that we used to isolate mollusc shell matrix proteins proceeds in two steps: fractionation of the shell matrix by preparative SDS-PAGE and assay of the isolated fractions on dot blots with an antibody elicited against the unfractionated matrix (37, 38). This allowed us to isolate two major proteins from the calcitic prismatic shell layer of the bivalve *P. nobilis*. We named these proteins caspartin and calprismismin, corresponding to the 17- and 38-kDa proteins, respectively.

Caspartin and calprismismin are two novel members of the small but rather disparate group of molluscan shell proteins that have been genetically or biochemically characterized (8, 9). This includes the twin proteins nacrein (73) and N66 (74), three framework proteins, MSI60, MSI31 (16), and MSI7 (75), the N14/N16/pearlin family (66, 74, 76), lustrin A (77), perlustrin (68, 78), mucoperlin (79), MSP-1 (80, 81), perlucin (67), a snail dermatopontin (82), AP7, and AP24 (83). This group also includes the recently found prismalin (17), aspein (18), asprich (19), and a histidine-rich protein of the extrapallial fluid (84). Furthermore, the shell protein group includes a few partly sequenced proteins (85–90).

Caspartin and calprismismin share many characteristics. They are soluble in acetic acid, and they are acidic due to their high Asx content. Their amino acid composition considerably deviates from the standard for proteins (91). Because these proteins are obtained after harsh treatment of the calcitic prisms with sodium hypochlorite, they are likely to be intimately associated with the mineral phase. Thus, in a first approximation, they could be described as *intracrystalline*. On a gel, they do not stain well and tend to migrate as diffuse bands. These two properties are usually found among proteins associated with calcified tissues (85, 86, 92). In denaturing conditions, neither caspartin nor calprismismin binds calcium. However, in the absence of Laemmli buffer, we demonstrated that caspartin, calprismismin, and the whole soluble matrix are able to bind calcium, although this effect is extremely reduced for calprismismin. A low affinity for calcium would be sufficient for temporarily sequestering calcium ions and releasing them when appropriate (93). Caspartin and calprismismin may act as crystal-binding rather than calcium-binding proteins (94). Our *in vitro* experiments suggest that at least caspartin strongly interacts with growing calcite crystals.

Despite a few similarities, caspartin and calprismismin are unlikely to belong to the same protein family. While caspartin seems to be a “true” aspartic acid-rich protein, calprismismin does not resemble any other calcifying protein. Contrary to caspartin, calprismismin is glycosylated. To date, only two shell proteins, the snail dermatopontin (82) and AP24 (83), have been shown to be glycosylated via asparagine. Because calprismismin stains well with Alcian blue but contains only low amounts of neutral and amino sugars, it is likely to carry acidic sugars, the chemical identity of which remains to be determined. Contrary to caspartin, calprismismin tends to smear when extracted from prisms of old specimens, and we suspect this protein to be rather labile. The fact that a small number of amino acids makes up the bulk of the molecule is characteristic of all proteins associated with biominerals (3, 95). On the other hand, the occurrence of proline and threonine is rather uncommon in this group. A potentially interesting feature comes from the cysteine pattern of calprismismin, which is similar to that found in granulins and in fungal surface glycoproteins. This may suggest that calprismismin might be involved in cell signaling or in matrix-cell interaction (14, 15, 96–98). However, because of its low level of homology and its incomplete characterization, the function of calprismismin is enigmatic.

In contrast to calprismismin, caspartin has more defined relation-

ships, since it may be included in the small group of aspartic acid-rich shell proteins. These soluble proteins, which were discovered by Weiner and co-workers (50, 95), are central to current hypotheses on molluscan mineralization, whereby they are thought to act as a template for nucleating calcium carbonate crystals (7, 12, 50). Initially, these proteins could not be easily isolated and characterized, so that their existence could only be inferred from amino acid composition and partial sequencing. The first members of this “family” to be described were three proteins extracted from the calcitic prismatic layer of the mussel *Mytilus californianus* (99, 100). RP-1 was another member from which short peptides were isolated and sequenced (85–87). More recently, the use of molecular biology techniques allowed the identification of transcripts, which encode putative Asp-rich proteins. The deduced protein sequences have been named MSP-1, aspein, and asprich. MSP-1 is an Asp-rich multidomain protein (80, 81) with a deduced molecular mass of 74.5 kDa. MSP-1 exhibits some similarities with phosphophoryns, a group of highly acidic proteins of the teeth (92, 101). The second fully sequenced transcript encodes aspein, the most acidic protein found to date (18). Aspein is a 39-kDa protein, which exhibits Asp_n blocks punctuated with Ser-Gly dipeptides. Asp, Ser, and Gly represent 90% of the composition of aspein. Caspartin differs markedly from MSP-1 and aspein, because it contains very few serine and glycine residues but more glutamic acid. In that respect, caspartin might have more affiliation with the third protein family, the “asprich” proteins, recently identified from 10 transcripts of *Atrina rigida* (19). Interestingly, *Atrina rigida* is a nacropismatic bivalve, which is closely related to *P. nobilis*. The molecular weights of asprich-proteins vary between 8.5 and 27 kDa, and their Asp content varies between 32 and 50%. Compared with caspartin, asprich proteins are enriched in Glu (6.2–12.9%), Ala (10.3–16.7%), Val (3.5–8.8%), and Ser (4.9–9.8%). Asprich proteins have only been deduced from their transcripts and not by biochemical methods after an extraction/purification procedure. It is therefore premature to group caspartin and asprich proteins in the same subfamily.

How are the calcitic prisms of *P. nobilis* formed? The mechanism by which prisms grow is still unclear and controversial. Computer simulations show that prism-like textures may be easily produced by competition of spherulites (102, 103). When growing spherulites, which are regularly nucleated on a plane, come into contact, they grow only in one direction and form elongated crystals. Competition for space has been put forward to explain the formation of composite prisms of Unionid bivalves (104, 105). In *P. nobilis*, the early steps of prism formation are characterized by the presence of spherulites (25, 106) on the inner surface of the periostracal layer. However, histological observations clearly show that the interprismatic walls are produced before the mineral phase is deposited (25). In this case, crystal growth by competition is not required, since the prisms grow within a preformed mold. This does not mean that prisms grow “passively.” Instead, prisms are likely to emerge from a complex interplay of electrostatic, stereochemical, and geometrical interactions (107).

Because caspartin is a major protein of the acetic acid-soluble matrix, it may play a central role in prism formation. We tentatively suggest the following functions. First, on growing prism surfaces, the intracrystalline caspartin would act as a local nucleator of CaCO₃ crystals. The nucleation surface of each prism would not be a continuous polyanionic film of caspartin but rather a surface punctuated by discrete caspartin spots, from which nanocrystals would grow and coalesce. Second, the caspartin film, which is anchored on the insoluble interprismatic walls, provides a strongly negatively charged environment. Thus, the honey-

comb-like framework, when coated with caspartin film, may be considered a polyanionic sink, which would help to attract and sequester calcium ions or to drive bicarbonate ions to the nucleating surface at the contact surface of the growing prisms and the supersaturated mother fluid. At the same time, the polyanionic envelope would act as an inhibitor constraining the outgrowth of the calcite crystals. Last, because caspartin polymerizes, the complex multimers formed may play a role in keeping a single crystallographic orientation of the prism nuclei, in such a way that each formed prism exhibits a single crystallographic orientation. Like other shell proteins, caspartin may be a multifunctional protein. More characterization (in particular sequence information and antisense RNA assays on larval fan mussels) is required before we can ascertain the function of caspartin in the formation of calcitic prisms.

Acknowledgments—Nicolas Navarro and Alain Godon (UMR 5561 "Biogéosciences") are acknowledged for help in designing Figs. 6, 8, and 9. F. Marin also thanks Claudie Josse (Laboratoire de Réactivité des Solides, Université de Bourgogne, Dijon, France) for help in handling the scanning electron microscope. F. Marin also thanks Prof. Nardo Vicente (CERAM, Marseille, France) for help in providing shell samples of *P. nobilis* and an anonymous reviewer for helpful corrections and suggestions.

REFERENCES

1. Simkiss, K., and Wilbur, K. M. (1989) *Biom mineralization: Cell Biology and Mineral Deposition*, Academic Press, London
2. Saleuddin, A. S. M., and Petit, H. P. (1983) in *The Mollusca* (Saleuddin, A. S. M., and Wilbur, K. M., eds) Vol. 4, pp. 199–234, Academic Press, Inc., New York
3. Lowenstam, H. A., and Weiner, S. (1989) *On Biom mineralization*, Oxford University Press, New York
4. Mann, S. (2001) *Biom mineralization: Principles and Concepts in Bioinorganic Material Chemistry*, Oxford University Press, London
5. Kaplan, D. L. (1998) *Curr. Opin. Solid State Mater. Sci.* **3**, 232–236
6. Belcher, A. M., and Gooch, E. E. (2000) in *Biom mineralization: From Biology to Biotechnology and Medical Applications* (Bauerlein, E., ed) pp. 221–249, Wiley-VCH, Weinheim, Germany
7. Weiner, S., Traub, W., and Lowenstam, H. A. (1983) in *Biom mineralization and Biological Metal Accumulation, Biological and Geological Perspectives* (Westbroek, P., and de Jong, E. W., eds) pp. 205–224, D. Reidel Publishing Co., Dordrecht, The Netherlands
8. Wilt, F. H., Killian, C. E., and Livingston, B. T. (2003) *Differentiation* **71**, 237–250
9. Marin, F., and Luquet, G. (2004) *C. R. Palevol.* **3**, 469–492
10. Currey, J. D. (1999) *J. Exp. Biol.* **202**, 3285–3294
11. Carter, J. G. (ed) (1990) *Skeletal Biom mineralization: Patterns, Processes and Evolutionary Trends*, Van Nostrand Reinhold, New York
12. Weiner, S., and Traub, W. (1984) *Phil. Trans. R. Soc. Lond. B* **304**, 425–434
13. Tisdell, C. A., and Poirine, B. (2000) *SPC Pearl Oyster Inform. Bull.* **14**, 21–31
14. Lopez, E., Berland, S., and Le Faou, A. (1995) *Bull. Inst. Océanogr. Monaco* **14**, 49–57
15. Westbroek, P., and Marin, F. (1998) *Nature* **392**, 861–862
16. Sudo, S., Fujikawa, T., Nagakura, T., Ohkubo, T., Sakaguchi, K., Tanaka, M., Nakashima, K., and Takahashi, T. (1997) *Nature* **387**, 563–564
17. Suzuki, M., Murayama, E., Inoue, H., Ozaki, N., Tohse, H., Kogure, T., and Nagasawa, H. (2004) *Biochem. J.* **382**, 205–213
18. Tsukamoto, D., Sarashina, I., and Endo, K. (2004) *Biochem. Biophys. Res. Commun.* **320**, 1175–1180
19. Gotliv, B. A., Kessler, N., Sumerel, J. L., Morse, D. E., Tuross, N., Addadi, L., and Weiner, S. (2005) *ChemBioChem* **6**, 304–314
20. Simkiss, K. (1968) in *Egg Quality: A Study of the Hen's Egg* (Carter, T. C., ed) pp. 3–25, Oliver & Boyd Ltd., Edinburgh
21. Gaspard, D. (1978) *Ann. Paléontol.* **64**, 1–25
22. Runnegar, B. (1985) *Alcheringa* **9**, 245–257
23. Kouchinsky, A. (2000) *Acta Palaeontol. Pol.* **45**, 119–150
24. Taylor, J. D., Kennedy, W. J., and Hall, A. (1969) *Bull. Br. Mus. Nat. Hist. Zool. Suppl.* **3**, 1–125
25. Cuif, J. P., Denis, A., and Raguideau, A. (1983) *Haliotis* **13**, 131–141
26. Cuif, J. P., Flamand, D., Frérotte, B., Chabin, A., and Raguideau, A. (1987) *C. R. Acad. Sci. (Paris) Sér. II* **304**, 475–478
27. Cuif, J. P., Gautret, P., and Marin, F. (1991) in *Mechanisms and Phylogeny of Mineralization in Biological Systems* (Suga, S., and Nakahara, H., eds) pp. 391–395, Springer-Verlag, Tokyo, Japan
28. Marin, F., Muzzer, G., and Dauphin, Y. (1994) *C. R. Acad. Sci. (Paris) Sér. II* **318**, 1653–1659
29. Dauphin, Y. (2002) *Comp. Biochem. Phys. B Biol. Sci.* **132**, 577–590
30. Dauphin, Y. (2003) *J. Biol. Chem.* **278**, 15168–15177
31. European Economic Community (1992) *Official Journal of the EU* **L206**, 0007–0050
32. Laemmli, U. K. (1970) *Nature* **227**, 680–685
33. Morrissey, J. H. (1981) *Anal. Biochem.* **117**, 307–310
34. Towbin, H., Staehelin, T., and Gordon, J. (1979) *Proc. Natl. Acad. Sci. U. S. A.* **76**, 4350–4354
35. Matsudaira, P. (1987) *J. Biol. Chem.* **262**, 10035–10038
36. Leong, M. M. L., Milstein, C., and Pannell, R. (1986) *J. Histochem. Cytochem.* **34**, 1645–1650
37. Marin, F., Pereira, L., and Westbroek, P. (2001) *Protein Expression Purif.* **23**, 175–179
38. Marin, F. (2003) *Scientific World J.* **3**, 342–347
39. Schuster, R. (1988) *J. Chromatogr.* **431**, 271–284
40. Campbell, K. P., MacLennan, D. H., and Jorgensen, A. O. (1983) *J. Biol. Chem.* **258**, 11267–11273
41. Maruyama, K., Mikawa, T., and Ebashi, S. (1984) *J. Biochem. (Tokyo)* **95**, 511–519
42. Wall, R. S., and Gyi, T. J. (1988) *Anal. Biochem.* **175**, 298–299
43. Devine, P. L., and Warren, J. A. (1990) *BioTechniques* **8**, 492
44. Edge, A. S. B., Faltynek, C. R., Hof, L., Reichert, L. E., and Weber, P. (1981) *Anal. Biochem.* **118**, 131–137
45. Hardy, M. R. (1989) *Methods Enzymol.* **179**, 76–82
46. Dionex Corp. (1998) *Technical Note* **40**, 1–6, Sunnyvale, CA
47. Wheeler, A. P., George, J. W., and Evans, C. A. (1981) *Science* **212**, 1397–1398
48. Albeck, S., Aizenberg, J., Addadi, L., and Weiner, S. (1993) *J. Am. Chem. Soc.* **115**, 11691–11697
49. Clark, M. F., and Adams, A. N. (1977) *J. Gen. Virol.* **34**, 475–483
50. Weiner, S., and Hood, L. (1975) *Science* **190**, 987–989
51. Krampitz, G., Drolshagen, H., Hausle, J., and Hof-Irmscher, J. (1983) in *Biom mineralization and Biological Metal Accumulation* (Westbroek, P., and De Jong, E. W., eds) pp. 231–247, D. Reidel Publishing Co., Dordrecht, The Netherlands
52. Marin, F., De Groot, K., and Westbroek, P. (2003) *Protein Expression Purif.* **30**, 246–252
53. Veis, A., Sabsay, B., and Wu, B. C. (1991) in *Surface Reactive Peptides and Polymers* (Sikes, C. S., and Wheeler, A. P., eds) pp. 1–12, American Chemical Society, Washington, D. C.
54. Nakahara, H., Kakei, M., and Bevelander, G. (1980) *Venus Jpn. J. Malacol.* **39**, 167–177
55. Albeck, S., Weiner, S., and Addadi, L. (1996) *Chem. Eur. J.* **2**, 278–284
56. Wilkins, M. R., Ou, K., Appel, R. D., Sanchez, J. C., Yan, J. X., Golaz, O., Farnsworth, V., Cartier, P., Hochstrasser, D. F., Williams, K. L., and Gooley, A. A. (1996) *Biochem. Biophys. Res. Commun.* **221**, 609–613
57. Takeuchi, K., Hatanaka, A., Kimura, M., Seki, N., Kimura, I., Yamada, S., and Yamashita, S. (2003) *J. Biol. Chem.* **278**, 47416–47422
58. Gattiker, A., Gasteiger, E., and Bairoch, A. (2002) *Appl. Bioinformatics* **1**, 107–108
59. Yazaki, P. J., Salvatori, S., and Dahms, A. S. (1990) *Biochem. Biophys. Res. Commun.* **170**, 1089–1095
60. Clegg, D. O., Helder, J. C., Hann, B. C., Hall, D. E., and Reichardt, L. F. (1988) *J. Cell Biol.* **107**, 699–705
61. Thanka Christlet, T. H., and Veluraja, K. (2001) *Biophys. J.* **80**, 952–960
62. Altschul, S. F., Madden, T. L., Schäffer, A. A., Zhang, J., Zhang, Z., Miller, W., and Lipman, D. J. (1997) *Nucleic Acids Res.* **25**, 3389–3402
63. Iozzo, R. V. (1997) *Crit. Rev. Biochem. Mol. Biol.* **32**, 141–174
64. Iozzo, R. V. (1998) *Annu. Rev. Biochem.* **67**, 609–652
65. Vitt, U. A., Hsu, S. Y., and Hsueh, A. J. W. (2001) *Mol. Endocrinol.* **15**, 681–694
66. Samata, T., Hayashi, N., Kono, M., Hasegawa, K., Horita, C., and Akera, S. (1999) *FEBS Lett.* **462**, 225–229
67. Mann, K., Weiss, I. M., André, S., Gabius, H. J., and Fritz, M. (2000) *Eur. J. Biochem.* **267**, 5257–5264
68. Weiss, I. M., Göhring, W., Fritz, M., and Mann, K. (2001) *Biochem. Biophys. Res. Commun.* **285**, 244–249
69. Blom, N., Gammeltoft, S., and Brunak, S. (1999) *J. Mol. Biol.* **294**, 1351–1362
70. Hansen, J. E., Lund, O., Tolstrup, N., Gooley, A. A., Williams, K. L., and Brunak, S. (1998) *Glycoconj. J.* **15**, 115–130
71. Huttner, W. B. (1987) *Trends Biochem. Sci.* **12**, 361–363
72. Armstrong, D. J., and Roman, A. (1993) *Biochem. Biophys. Res. Commun.* **192**, 1380–1387
73. Miyamoto, H., Miyashita, T., Okushima, M., Nakano, S., Morita, T., and Matsushiro, A. (1996) *Proc. Natl. Acad. Sci. U. S. A.* **93**, 9657–9660
74. Kono, M., Hayashi, N., and Samata, T. (2000) *Biochem. Biophys. Res. Commun.* **269**, 213–218
75. Zhang, Y., Xie, L., Meng, Q., Jiang, T., Pu, R., Chen, L., and Zhang, R. (2003) *Comp. Biochem. Phys. B Biol. Sci.* **135**, 565–573
76. Miyashita, T., Takagi, R., Okushima, M., Nakano, S., Miyamoto, H., Nishikawa, E.,

Characterization of Two Shell Proteins from Calcitic Prisms

- and Matsushiro, A. (2000) *Mar. Biotechnol.* **2**, 409–418
77. Shen, X., Belcher, A. M., Hansma, P. K., Stucky, G. D., and Morse, D. E. (1997) *J. Biol. Chem.* **272**, 32472–32481
78. Weiss, I. M., Kaufmann, S., Mann, K., and Fritz, M. (2000) *Biochem. Biophys. Res. Commun.* **267**, 17–21
79. Marin, F., Corstjens, P., De Gaulejac, B., De Vrind-De Jong, E., and Westbroek, P. (2000) *J. Biol. Chem.* **275**, 20667–20675
80. Sarashina, I., and Endo, K. (1998) *Am. Mineral* **83**, 1510–1515
81. Sarashina, I., and Endo, K. (2001) *Mar. Biotechnol.* **3**, 362–369
82. Marxen, J. C., Nimtz, M., Becker, W., and Mann, K. (2003) *Biochim. Biophys. Acta* **1650**, 92–98
83. Michenfelder, M., Fu, G., Lawrence, C., Weaver, J. C., Wustman, B. A., Taranto, L., Evans, J. S., and Morse, D. E. (2003) *Biopolymers* **70**, 522–533
84. Hattan, S. J., Laue, T. M., and Chasteen, N. D. (2001) *J. Biol. Chem.* **276**, 4461–4468
85. Rusenko, K. W., Donachy, J. E., and Wheeler, A. P. (1991) *Am. Chem. Soc. Symp. Ser.* **444**, 107–124
86. Donachy, J. E., Drake, B., and Sikes, C. S. (1992) *Mar. Biol.* **114**, 423–428
87. Halloran, B. A., and Donachy, J. E. (1995) *Comp. Biochem. Phys. B Biol. Sci.* **111**, 221–231
88. Bédouet, L., Schuller, M. J., Marin, F., Milet, C., Lopez, E., and Giraud, M. (2001) *Comp. Biochem. Phys. B Biol. Sci.* **128**, 389–400
89. Keith, J., Stockwell, S., Ball, D., Remillard, K., Kaplan, D., Thannhauser, T., and Sherwood, R. (1993) *Comp. Biochem. Phys. B Biol. Sci.* **105**, 487–496
90. Marxen, J. C., and Becker, W. (1997) *Comp. Biochem. Phys. B Biol. Sci.* **118**, 23–33
91. McCaldon, P., and Argos, P. (1988) *Proteins* **4**, 99–122
92. Stetler-Stevenson, W. G., and Veis, A. (1983) *Biochemistry* **22**, 4326–4335
93. Mann, S. (1988) *Nature* **332**, 119–124
94. Wheeler, A. P., Rusenko, K. W., George, J. W., and Sikes, C. S. (1987) *Comp. Biochem. Phys. B Biol. Sci.* **87**, 953–960
95. Weiner, S. (1979) *Calcif. Tissue Int.* **29**, 163–167
96. Reddi, A. H. (2000) *Biochem. Soc. Trans.* **28**, 345–349
97. Almeida, M. J., Milet, C., Peduzzi, J., Pereira, L., Haigle, J., Barthelemy, M., and Lopez, E. (2000) *J. Exp. Zool.* **288**, 327–334
98. Bateman, A., and Bennett, H. P. J. (1998) *J. Endocrinol.* **158**, 145–151
99. Weiner, S. (1983) *Biochemistry* **22**, 4139–4144
100. Addadi, L., Moradian, J., Shay, E., Maroudas, N. G., and Weiner, S. (1987) *Proc. Natl. Acad. Sci. U. S. A.* **84**, 2732–2736
101. Ritchie, H. H., and Wang, L. H. H. (1996) *J. Biol. Chem.* **271**, 21695–21698
102. Ubukata, T. (1994) *Palaeontology* **37**, 241–261
103. Ubukata, T. (1997) *Veliger* **40**, 165–177
104. Checa, A. (2000) *Tissue Cell* **32**, 405–416
105. Checa, A., and Rodriguez-Navarro, A. (2001) *Proc. R. Soc. Lond. B* **268**, 771–778
106. Dauphin, Y., Cuif, J. P., Doucet, J., Salomé, M., Susini, J., and Williams, C. T. (2003) *J. Struct. Biol.* **142**, 272–280
107. Heywood, B. R., and Mann, S. (1994) *Adv. Mater.* **6**, 9–20

Caspartin and Calprismin, Two Proteins of the Shell Calcitic Prisms of the Mediterranean Fan Mussel *Pinna nobilis*
Frédéric Marin, Reinout Amons, Nathalie Guichard, Martin Stigter, Arnaud Hecker, Gilles Luquet, Pierre Layrolle, Gérard Alcaraz, Christophe Riondet and Peter Westbroek

J. Biol. Chem. 2005, 280:33895-33908.

doi: 10.1074/jbc.M506526200 originally published online July 1, 2005

Access the most updated version of this article at doi: [10.1074/jbc.M506526200](https://doi.org/10.1074/jbc.M506526200)

Alerts:

- [When this article is cited](#)
- [When a correction for this article is posted](#)

[Click here](#) to choose from all of JBC's e-mail alerts

This article cites 97 references, 17 of which can be accessed free at <http://www.jbc.org/content/280/40/33895.full.html#ref-list-1>